

## Title Page

# Exploring the Pharmacokinetic Mysteries of the Liver: Application of Series Compartment Models of Hepatic Elimination

Xiaonan Li and William J. Jusko\*

Department of Pharmaceutical Sciences, State University of New York at Buffalo, 404 Pharmacy Building, Buffalo, New York 14214, USA

## Running Title Page

Series Compartment Models of Hepatic Elimination

### \* Corresponding author

William J. Jusko, PhD

Department of Pharmaceutical Sciences, State University of New York at Buffalo, 404 Pharmacy  
Building, Buffalo, New York 14214, USA

E-mail: [wjjusko@buffalo.edu](mailto:wjjusko@buffalo.edu)

Number of text pages: 42

Number of tables: 3

Number of figures: 9

Number of references: 66

Number of words in Abstract: 224

Number of words in Introduction: 751

Number of words in Discussion: 1994

## ABBREVIATIONS

$AUC$ , area under the curve;  $CL_b$ , total blood clearance;  $CL_h$ , hepatic clearance;  $CL_{int}$ , hepatic intrinsic clearance;  $C_{max}$ , maximum concentration; CyA, cyclosporine A; DLZ, diltiazem;  $D_N$ , dispersion number; DM, dispersion model; DZP, diazepam; EB, ethoxybenzamide; ER, extraction ratio;  $F$ , hepatic availability; FTY720, fingolimod;  $f_{ub}$ , unbound fraction in blood; IV, intravenous; IVIVE, *in vitro*-to-*in vivo* extrapolation;  $K_p$ , tissue-to-plasma partition coefficient;  $n$ , number of liver sub-compartments; PBPK, physiologically-based pharmacokinetic; PD, pharmacodynamic; PK, pharmacokinetic; PTM, parallel tube model;  $R_b$ , blood-to-plasma ratio; SS, steady state;  $T_{max}$ , time to reach  $C_{max}$ ; VEM, verapamil; WSM, well-stirred model.

## Abstract

Among the basic hepatic clearance models, the dispersion model (DM) is the most physiologically sound compared to the well-stirred model (WSM) and the parallel tube model (PTM). However, its application in physiologically-based pharmacokinetic (PBPK) modeling has been limited due to computational complexities. The series compartment models (SCM) of hepatic elimination that treats the liver as a cascade of well-stirred compartments connected by hepatic blood flow exhibits some mathematical similarities to the DM but is easier to operate. This work assesses the quantitative correlation between the SCM and DM and demonstrates the operation of the SCM in PBPK with the published single-dose blood and liver concentration-time data of 6 flow-limited compounds. The predicted liver concentrations and the estimated intrinsic clearance ( $CL_{int}$ ) and PBPK-operative tissue-to-plasma partition coefficient ( $K_p$ ) values were shown to depend on the number of liver sub-compartments ( $n$ ) and hepatic enzyme zonation in the SCM. The  $CL_{int}$  and  $K_p$  decreased with increasing  $n$ , with more remarkable differences for drugs with higher hepatic extraction ratios ( $ER$ ). Given the same total  $CL_{int}$ , the SCM yields a higher  $K_p$  when the liver perivenous region exhibits a lower  $CL_{int}$  as compared to a high  $CL_{int}$  at this region. Overall, the SCM nicely approximates the DM in characterizing hepatic elimination and offers an alternative flexible approach as well as providing some insights regarding sequential drug concentrations in the liver.

**Keywords** Series compartment models; Hepatic clearance models; Hepatic enzyme zonation; Physiologically-based pharmacokinetic modeling; Intrinsic clearance; Tissue-to-plasma partition coefficient

## Significance Statement

The SCM nicely approximates the DM when applied in PBPK for characterizing hepatic elimination. The number of liver sub-compartments and hepatic enzyme zonation are influencing factors for the SCM resulting in model-dependent predictions of total/internal liver concentrations and estimates of  $CL_{int}$  and the PBPK-operative  $K_p$ . Such model-dependency may have an impact when the SCM is used for *in vitro*-to-*in vivo* extrapolation (IVIVE) and may also be relevant for PK/PD/toxicological effects when it is the driving force for such responses.

## Introduction

The pharmacokinetic (PK) field has sought to elucidate the properties and mechanisms of drug distribution and elimination in the liver as it serves as the major clearance organ. Various liver-derived *in vitro* metabolic systems (microsomes, hepatocytes, homogenates, slices) have been used for prediction of *in vivo* hepatic clearance ( $CL_h$ ) using the measured intrinsic clearance ( $CL_{int}$ ) (viz. *in vitro*-to-*in vivo* extrapolation, IVIVE). On the other hand, physiologically-based PK (PBPK) modeling allows for characterizing dynamic changes in hepatic concentrations in pre-clinical species and scaling-up to humans (Lee et al., 2020) where the  $CL_{int}$  and tissue-to-plasma partition coefficient ( $K_p$ ) are needed. Both IVIVE and PBPK modeling require a structural liver model (Rane et al., 1977; Houston, 1994; Hallifax et al., 2010; Miller et al., 2019). The primary hepatic models are the well-stirred (WSM), parallel tube (PTM), and dispersion models (DM) (Rowland et al., 1973; Pang and Rowland, 1977; Roberts and Rowland, 1986a; Roberts and Rowland, 1986b; Pang et al., 2019; Jusko and Li, 2021; Li and Jusko, 2022). Their assumed internal flow and mixing patterns differ, with the degree of longitudinal or axial dispersion of a solute passing through the liver characterized by the dispersion number ( $D_N$ ). The WSM has infinite mixing of blood ( $D_N = \infty$ ) and uniform intrahepatic and outflow blood concentrations while the PTM exhibits no mixing ( $D_N = 0$ ) and a mono-exponential concentration decline. The DM features intermediate mixing or dispersion ( $0 < D_N < \infty$ ) rendering a continuous concentration decline lying between those of the WSM and PTM. The average intrahepatic blood concentration ranking is WSM<DM<PTM, with the corresponding  $CL_{int}$  being opposite to achieve the same hepatic extraction ratio ( $ER$ ).

The utilization of these models in PBPK has been limited to the least physiological WSM largely owing to its computational simplicity. The use of the more physiologically sound DM in PBPK

is complicated as second-order partial differential equations are required (Oliver, 1995; Oliver et al., 2001). The DM is based on the residence time distribution of solutes reflecting the degree of dispersion (Levenspiel, 1999).

Another model to approximate complex flow and reaction systems is the “tanks-in-series” or “series compartment” model (SCM) where the liver is viewed as a cascade of identical well-stirred compartments connected by hepatic blood flow (Figure 1). The SCM is mathematically similar to the gamma distribution function describing the residence time distribution of a tracer exiting an organ (Buffham and Gibilaro, 1968; Davenport, 1983) and therefore equally well represents indicator-dilution curves (Goresky et al., 1973) as does the DM (Roberts and Rowland, 1986a; Gray and Tam, 1987). The SCM functioning is intermediate between the WSM and PTM and mimics the DM but is mathematically simpler. The degree of mixing in the SCM is determined by the number of liver sub-compartments ( $n$ ); the SCM predicts the same hepatic availability ( $F$ ) as the WSM when  $n = 1$  and gives approximately equal  $F$  values to the PTM when  $n > 30$  (Gray and Tam, 1987).

A zonal-compartment model, a modified version of the SCM, considers enzyme zonal heterogeneity, where the liver is divided into three zones with different metabolic activities, i.e., periportal (PP), midzonal, and perivenous (PV) regions (Tirona and Pang, 1996; Abu-Zahra and Pang, 2000). The SCM was also extended to characterize the disposition of pravastatin where the liver was divided into five sequential units of extracellular and subcellular compartments to include transporters (Watanabe et al., 2009). The selection of 5 liver sub-compartments was primarily based on how it predicts the closest  $F$  value of pravastatin as given by the DM. This complex SCM was applied to other substrates of hepatic transporters (Jones et al., 2012; Li et al., 2014; Li et al., 2016; Morse et al., 2017). Recently, the SCM with varying  $n$  was used to assess

the correlation between *in vitro* and *in vivo* unbound liver-to-plasma partition coefficients ( $K_{puu}$ ); however, their analysis was limited to algebraic equations derived under steady-state (SS) conditions (Li et al., 2019).

Although the SCM was claimed to closely approximate the DM, their quantitative correlations have not been explored. It remains unclear how the choice of  $n$  and hepatic enzyme zonation affect the estimation of  $CL_{int}$  and  $K_p$  as well as model predictions of internal liver concentration-time profiles. We herein consider these aspects by incorporating the basic hepatic SCM (Gray and Tam, 1987) into PBPK with characterization of published single-dose blood/plasma and liver concentration-time data from rats for 6 flow-limited compounds primarily cleared by the liver. This report will also serve as a tutorial on operating the SCM in PBPK modeling.

## Methods

The SCM of hepatic elimination is displayed in Figure 1, where the liver is divided into  $n$  well-stirred sub-compartments connected by hepatic blood flow. Each of the sub-compartments was assumed to equally share the same total tissue volume ( $V_h$ ), availability ( $F$ ), extraction ratio ( $ER$ ), and intrinsic clearance ( $CL_{int}$ ). Thus, for the  $i$ th ( $i=1, 2, 3 \dots n$ ) compartment:

$$V_{hi} = \frac{V_h}{n} \quad (1)$$

$$F_i = \sqrt[n]{1 - ER} \quad (2)$$

$$ER_i = 1 - F_i \quad (3)$$

$$f_{ub}CL_{inti} = \frac{Q_h ER_i}{1 - ER_i} \quad (4)$$

$$f_{ub}CL_{int} = n f_{ub}CL_{inti} \quad (5)$$

where  $C_h$  is the total liver concentration, and  $f_{ub}$  is the unbound fraction in blood.

The outflow blood concentration from the compartment  $i$  ( $C_{outi}$ ,  $i=1, 2, 3 \dots n$ ) is the input function for the subsequent compartment  $i+1$  and is assumed to be in equilibrium with the tissue concentration throughout the  $i$ th compartment ( $C_{hi}$ ,  $i=1, 2, 3 \dots n$ ) with each of the liver sub-compartments sharing the same liver-to-plasma concentration ratio  $K_p$ :

$$K_p = \frac{R_b C_{hi}}{C_{outi}} \quad (6)$$

where  $R_b$  is the blood-to-plasma ratio.

Therefore:

$$C_{outi} = \frac{R_b C_{hi}}{K_p} \quad (7)$$

The concentration changes in the 1<sup>st</sup> and  $i$ th well-stirred liver compartments are described by:

$$V_{h1} \frac{dC_{h1}}{dt} = Q_h (C_{in} - C_{out1}) - f_{ub}CL_{int1} \frac{R_b C_{h1}}{K_p} \quad (8)$$

and



$$V_{hi} \frac{dC_{hi}}{dt} = Q_h (C_{out(i-1)} - C_{outi}) - f_{ub} CL_{inti} \frac{R_b C_{hi}}{K_p}, \quad i=2, 3 \dots n \quad (9)$$

where  $C_{in}$  is the input blood concentration into the 1<sup>st</sup> liver compartment.

The total liver concentration is assumed to be the average of  $C_{hi}$  ( $i=1, 2, 3 \dots n$ ) in all compartments:

$$C_h = \frac{1}{n} \sum_{i=1}^n C_{hi} \quad (10)$$

### Model Simulations of $ER$ vs $CL_{int}$ : Comparing the SCM with the Basic Hepatic Clearance Models

The mathematical expression of  $ER$  for the SCM with  $n$  liver sub-compartments was derived from Eq. 2-5 as follows:

$$ER = 1 - \left( \frac{Q_h}{Q_h + \frac{f_{ub} CL_{int}}{n}} \right)^n \quad (11)$$

The relationships between  $ER$  and  $CL_{int}$  have been reported for the basic hepatic clearance models (Roberts and Rowland, 1986a; Roberts and Rowland, 1986b). For the DM based on the closed boundary conditions ( $0 < Z < 1$ , where  $Z$  is defined as the distance along the length of the liver):

$$ER = 1 - \frac{4a}{(1+a)^2 e^{(a-1)/2D_N} - (1-a)^2 e^{-(a+1)/2D_N}} \quad (12)$$

where  $a = (1+4D_N R_N)^{1/2}$  and  $R_N$ , the efficiency number that measures the removal rate of substances by liver cells, is given by:

$$R_N = \frac{f_{ub} CL_{int}}{Q_h} \quad (13)$$

The mathematical expression of  $ER$  for the WSM can be derived from that of the SCM (Eq.11) by setting  $n = 1$ , and from that of the DM (Eq.12) with  $D_N = \infty$ :

$$ER = \frac{f_{ub} CL_{int}}{Q_h + f_{ub} CL_{int}} \quad (14)$$

Similarly, the mathematical expression of ER for the PTM is equivalent to that of the SCM (Eq.11) with  $n = \infty$  and the DM (Eq.12) with  $D_N = 0$ :

$$ER = 1 - e^{-\frac{f_{ub}CL_{int}}{Q_h}} \quad (15)$$

To assess the quantitative similarities between the SCM and the basic hepatic clearance models, the relationships between  $ER$  and  $CL_{int}$  were simulated according to Eq.11, 12, 14, and 15 with varying values of  $n$  for the SCM and  $D_N$  for the DM. For the DM, the commonly reported range of  $D_N$  (0.1~0.6) (Diaz-Garcia et al., 1992; Chou et al., 1993; Evans et al., 1993; Oliver et al., 2001) was applied and  $f_{ub}$  was assumed to be 1 in all simulations for simplicity.

### **Assessing Liver $CL_{int}$ and $K_p$ by the SCM of Hepatic Elimination in PBPK**

The measured blood or plasma and liver concentration-time data in rats after single intravenous (IV) bolus doses were obtained from the literature for 6 compounds including cyclosporine A (CyA) (Kawai et al., 1998), ethoxybenzamide (EB) (Lin et al., 1978), fingolimod (FTY720) (Meno-Tetang et al., 2006), diazepam (DZP) (Igari et al., 1983), verapamil (VEM) (Yamano et al., 2000), and diltiazem (DLZ) (Yamano et al., 2000). Concentration versus time data were digitized from the published graphs using GetData Graph Digitizer version 2.26 (<http://getdata-graph-digitizer.com/>). These model compounds were selected based on the following conditions:

- Liver is the major eliminating organ
- Extrahepatic clearances are known or assumed to be negligible
- Tissue-to-plasma concentration ratios are linear
- ER ranges from low to high
- Time courses of blood/plasma and liver concentrations are resolvable
- Distribution into the liver and access to the hepatic enzymes are flow-limited (high permeability) with minor or negligible transporter involvement

As was similarly done previously (Ebling et al., 1994; Foster, 1998; Gueorguieva et al., 2004; Cheung et al., 2018; Li and Jusko, 2022), a piecewise open-loop approach was applied. Briefly, the blood concentration ( $C_b$ )-time profile was fitted first and then used as the forcing input function (i.e., replacing the  $C_{in}$  term in Eq. 8 by the fitted  $C_b$ ) to model the concentration-time data of the liver as a single organ. This method was advantageous for our purposes as we did not have to deal with involvement of organs/tissues other than the liver and it was also reported to generate comparable hepatic  $K_p$  estimates as obtained by fitting all tissues simultaneously using a full PBPK model (Gueorguieva et al., 2004).

The exponential equations used to describe the  $C_b$ -time data are:

$$C_b = \begin{cases} Ae^{-\alpha t} + Be^{-\beta t} \\ Ae^{-\alpha t} + Be^{-\beta t} + Ce^{-\gamma t} \end{cases} \quad C_{b0} = Dose/V_b \quad (16)$$

where  $A$ ,  $B$ ,  $C$  are the intercepts,  $\alpha$ ,  $\beta$ ,  $\gamma$  are the slopes,  $C_{b0}$  is the initial blood concentration at time 0, and  $V_b$  is the average value of the reported blood volumes in the source literature (78 mL/kg).

Subsequently, the total blood clearance ( $CL_b$ ) can be obtained from:

$$CL_b = \frac{Dose}{AUC_b} \quad (17)$$

By assuming liver is the only clearance organ ( $CL_b = CL_h$ ),  $ER$  is given by:

$$ER = \frac{CL_b}{Q_h} \quad (18)$$

where  $Q_h = 60.82$  mL/min/kg and  $V_h = 36.6$  mL/kg are published values for rats (Brown et al., 1997).

For the SCM,  $f_{ub}CL_{inti}$  can be calculated from  $ER$  by rearranging Eq. 11:

$$f_{ub}CL_{inti} = \frac{Q_h \sqrt[n]{1-ER}}{\sqrt[n]{1-ER}}, \quad i = 1, 2 \dots n \quad (19)$$

Due to the limitation of the open-loop approach that  $CL_{int}$  and  $K_p$  are highly correlated yielding extremely large CV% values when estimated simultaneously, the  $CL_{int}$  of the SCM containing different  $n$  were first obtained using Eq. 17-19 with the  $CL_b$  and  $ER$  estimated from fitting the blood PK data and then fixed in the subsequent fitting of liver concentration-time data to estimate the PBPK-operative  $K_p$  according Eq.7-10, with  $C_{in}$  in Eq.8 being replaced by the pre-fitted  $C_b$  in Eq.16. The outflow blood concentration ( $C_{out,i}$ ,  $i=n$ ) from the last liver segment was calculated from the corresponding liver concentration ( $C_{hi}$ ,  $i=n$ ) according to Eq. 7 and the concentration-time profile in each of the liver sub-compartments was also simulated based on Eqs. 8-9.

### **Assessing Effects of Hepatic Enzyme Zonation on $K_p$ Estimation and Prediction of Liver Concentrations by the SCM**

The hepatic zonal heterogeneity of key metabolizing enzymes has been reviewed and its potential effects on hepatic metabolism of xenobiotics have been assessed by various *in vitro* and *in situ* liver-derived systems (Jungermann and Katz, 1989; Jungermann, 1995; Tirona and Pang, 1996; Oinonen and Lindros, 1998; Abu-Zahra and Pang, 2000; Li et al., 2019; Tomlinson et al., 2019). To assess how such hepatic zonation affects the estimation of liver  $K_p$  and the prediction of liver concentrations by PBPK models, uneven zonal-enzyme distribution (i.e., different  $ER_i$  and  $CL_{inti}$ ) was assumed for each of the sub-compartments in the SCM with  $n=5$ . The following scenarios were tested: (1) lower  $ER/CL_{int}$  at the PP region by assuming  $F_{i+1} = F_i^2$  ( $i=1, 2...4$ ), and (2) lower  $ER/CL_{int}$  at the PV region by assuming  $F_{i+1} = F_i^{1/2}$  ( $i=1, 2...4$ ). The results were compared with those previously obtained by assuming equal  $ER/CL_{int}$  for all liver segments.

For testing Scenario 1, the availability of the 1<sup>st</sup> and subsequent liver compartments are:

$$F_1 = \sqrt{(1+2+4+8+16)(1-ER)} \quad (20)$$

$$F_{i+1} = F_i^2, \quad i = 1, 2 \dots 4 \quad (21)$$

For testing Scenario 2, the availability of the 1<sup>st</sup> and subsequent liver compartments are:

$$F_1 = \sqrt{(1 + \frac{1}{2} + \frac{1}{4} + \frac{1}{8} + \frac{1}{16})} \sqrt{(1 - ER)} \quad (22)$$

$$F_{i+1} = F_i^{\frac{1}{2}}, \quad i = 1, 2 \dots 4 \quad (23)$$

With the assumed  $F_i$  values, the corresponding  $CL_{inti}$  can be obtained by Eq. 3 and 4 for the subsequent model fittings of liver data and the estimation of  $K_p$  using Eq. 7-10. Provided the relationship of  $F_{(i+1)} = F_i^a$  ( $i=1, \dots, n-1$ ), larger values of  $a$  produce steeper gradients of the metabolic clearance within the liver. By assigning a wide range of  $a$  values from 1~1000, the impact of steepness in the internal metabolic clearance gradients on the estimation of total  $CL_{int}$  and  $K_p$  by the 2- and 5-compartment zonal SCM was further assessed under testing Scenario 1.

### Model Fitting

The model fittings of blood and liver concentration-time data were performed by nonlinear regression using the maximum likelihood algorithm in ADAPT 5 (Biomedical Simulations Resources, Los Angeles, CA) (D'Argenio et al., 2009). The variance model was:

$$V_i = (\sigma_{inter} + \sigma_{slope} Y_i)^2 \quad (24)$$

where  $V_i$  is the variance of the  $i$ th data point;  $Y_i$  is the  $i$ th model-predicted concentration;  $\sigma_{inter}$  and  $\sigma_{slope}$  are the variance model parameters. Model selection was based on the goodness-of-fit criteria, which included the Akaike Information Criterion (AIC), visual inspection of the fitted profiles, and CV% of the parameter estimates.

The maximum predicted liver concentration ( $C_{max}$ ), time to reach  $C_{max}$  ( $T_{max}$ ), and area under the curve (AUC) of the predicted liver concentration-time data were obtained by non-compartmental

analysis (NCA) performed using Phoenix® WinNonlin® version 6.4 (Certara USA, Inc., Princeton, NJ).

The ADAPT code for the SCM model for one compound (DLZ) is provided in the Supplemental Methods.

## Results

### Simulations of $ER$ vs $CL_{int}$ as a Function of “ $n$ ” and “ $D_N$ ”: Comparing the SCM with Basic Hepatic Clearance Models

The simulated  $ER$  vs  $CL_{int}$  profiles using the SCM with varying values of  $n$  and the three basic hepatic clearance models are displayed in Figure 2. For the DM, the commonly reported  $D_N$  range of 0.1~0.6 was used for the model simulations with only the results obtained from the boundary values (i.e., 0.1 and 0.6) presented as any  $D_N$  value in between will yield intermediate profiles.

As expected, the  $ER$  increases with increasing  $CL_{int}$  for all models, with the SCM and DM exhibiting intermediate profiles that lie in between those of the PTM and WSM. With the same  $CL_{int}$ ,  $ER$  values given by the SCM increase with increasing  $n$  while the DM yields lower  $ER$  as  $D_N$  increases. To achieve the same  $ER$ , the rank order of  $CL_{int}$  is WSM>DM/SCM>PTM. The  $ER$  vs  $CL_{int}$  profile of the SCM is identical to that of the WSM when  $n = 1$  and becomes approximately equal to that of the PTM when  $n > 30$ , consistent with the previous report (Gray and Tam, 1987).

As can be seen from Figure 2, the simulated  $ER$  profiles using the SCM containing 2 and 5 liver sub-compartments closely match those of the DM with  $D_N$  equal to 0.6 and 0.1. Therefore, the SCM containing 1 (viz. the basic WSM), 2, and 5 liver sub-compartments were further utilized and compared in the subsequent fitting of liver data and estimation of  $CL_{int}$  and  $K_p$ .

### Assessing Liver $CL_{int}$ and $K_p$ in PBPK Models by the SCM: Exploring the Impact of $n$

With the open-loop approach, the  $C_b$ -time data were first characterized by Eq.16 with model fittings displayed in Figure 3. The estimates of intercepts and slopes are listed in Table S1. Secondary parameters are shown in Table 1, where  $CL_b$  and  $ER$  were estimated by Eqs.17-18,

and  $f_{ub}CL_{int}$  of the SCM with different values of  $n$  were obtained using Eq.19 with the  $ER$  estimated from fitting the blood PK data. The  $C_b$ -time profiles of all model compounds are well described by the exponential equations and parameter estimates exhibit low CV% values. In line with the model simulations in Figure 2, the estimated  $f_{ub}CL_{int}$  decreases with increasing  $n$  given the same  $ER$  especially for drugs with higher  $ER$  values (Table 1).

Subsequently, with the estimated  $f_{ub}CL_{int}$  and the fitted  $C_b$ -time profile as the forcing input function into the 1<sup>st</sup> liver sub-compartment (replacing  $C_{in}$  in Eq.8) of the SCM, liver  $K_p$  were obtained by fitting the measured  $C_h$ -time data using the SCM with  $n$  equal to 1, 2, and 5 (Eq.7-10). The model fittings are presented in Figure 3, and the estimated  $K_p$  as well as the AIC values for each of the models are listed in Table 1. Overall, the fitted  $C_h$ -time profiles by the SCM of different  $n$  exhibit slight differences at early time points while later concentrations were fitted equally well as the basic WSM (i.e.,  $n=1$ ) (Figure 3). As shown in Table 1, the selection of  $n$  shows little influence on the estimation of  $K_p$  for drugs with low  $ER$  (e.g., EB and CyA), however, the model-dependencies in  $K_p$  become more remarkable as  $ER$  increases. For the same compound, the SCM with larger  $n$  yields smaller  $K_p$  values. Such model dependency is in accordance with that of the  $CL_{int}$  (Figure 2 and Table 1). The similar AIC values suggest that model performance of the SCM in describing the measured liver data is not significantly affected by the selection of  $n$ . In line with the theoretical correlations (Figure 2), the parameter estimates obtained by the 2-segment SCM are comparable to those yielded by the DM with  $D_N=0.6$  from our previous analysis (Li and Jusko, 2022), viz, the  $CL_{int}$  and  $K_p$  values for DLZ are 211.9 mL/min/kg and 14.11 for the SCM, and 213 mL/min/kg and 13.96 for the DM.

The NCA was performed to obtain the maximum concentration ( $C_{max}$ ), time to reach  $C_{max}$  ( $T_{max}$ ), and area under the curve from time 0 to infinity ( $AUC_{inf}$ ) of the fitted liver concentration-time



data, and the relative changes in these parameters are provided to examine the differences in model predictions in relation to  $n$  (Table 2). As indicated by Figure 3 and Table 2, the predicted liver  $C_{max}$  of all compounds increases with increasing  $n$ , while the  $T_{max}$  are delayed for some of the compounds (e.g., FTY720, VEM and DLZ); the  $AUC_{inf}$  values are mostly comparable except for that of DZP which slightly increased with increasing  $n$ .

To explore the characteristics of intrahepatic drug disposition with the SCM, the concentration ( $C_{hi}$ )-time profiles in each of the liver sub-compartments were simulated and displayed in Figure 4. The SCM predicts an intrahepatic concentration gradient from the first to the last liver sub-compartment, which is quantitatively consistent with the theoretical expectations (Kashiwagi et al., 1981), and the magnitude of such concentration gradients was shown to be dependent on both the values of  $n$  and  $ER$  (Figure 4). For both the 2- and 5-compartment SCM, the  $C_{hi}$ -time curves shift to the right (delayed  $T_{max}$ ) with decreasing  $C_{max}$  values as  $i$  increases, exhibiting the typical profiles similar to those of transit compartment models (Sun and Jusko, 1998).

To assess whether the time delays in the intrahepatic concentrations are dependent on the selection of  $n$ , the concentration of DLZ in the venous blood leaving the last liver sub-compartment ( $C_{outn}$ ,  $n = 1, 2$ , and  $5$ ) was calculated from the corresponding liver concentration ( $C_{hn}$ ,  $n = 1, 2$ , and  $5$ ) and the estimated  $K_p$  (Table 1) using Eq. 7. As shown in Figure 5, the  $T_{max}$  of the  $C_{outn}$ -time profile increases with increasing values of  $n$ , which is 0.97 min ( $n=1$ ), 2.42 min ( $n=2$ ) and 4.23 min ( $n=5$ ), suggesting similar features of the SCM in characterizing time delays as transit compartment models. Such delays in  $T_{max}$  with increasing  $n$  were also observed for all the other tested compounds (Figure S1). Since  $C_{out}$  from the last liver sub-compartment is one of the input functions into the venous blood pool, such delays associated with the selection of  $n$

may be more relevant if the SCM is used in a full PBPK model even though the model fittings of total liver concentrations were similar (Figure 3 and Table 2).

### **Effects of Metabolic Zonation on Characterizing Liver Concentration-Time Data and Estimating $CL_{int}$ and $K_p$ by the SCM in PBPK**

The effects of hepatic enzyme zonation were assessed using the SCM containing 5 sub-compartments with the data for DLZ. To keep the  $ER$  of DLZ (Table 1) unchanged for different models, it is mathematically convenient to assign the assumed patterns of hepatic enzyme zonation based on the  $F$  value in each of the sub-compartments rather than the value of  $CL_{int}$  as was done previously (Li et al., 2019). Provided the relationship of  $F_{i+1}=F_i^a$  ( $i=1, \dots, n-1$ ), the exponential of  $F_i$ ,  $a$  was set to be 2 meaning increased metabolic clearance from the PP to PV region (Scenario 1) and 0.5 reflecting decreased metabolic clearance along the sinusoidal flow path (Scenario 2). This yielded an approximately 100-fold difference between the lowest and highest intrinsic clearances. In all testing scenarios, the  $f_{ub}CL_{inti}$  value was first obtained using the total  $ER$  based on Eq. 3-4 and 20-23. The calculated  $f_{ub}CL_{inti}$  (Table 3) and the pre-estimated blood PK parameters of DLZ (Table S1) were fixed in the subsequent model fitting of liver data according to Eq. 7-10. The model fittings utilizing two different testing scenarios were compared to those with an even distribution of enzymatic activity throughout the liver (Figure 6). The estimated  $K_p$  along with the  $T_{max}$ ,  $C_{max}$ , and  $AUC_{inf}$  values of the fitted liver profiles are listed in Table 3.

The estimated total  $CL_{int}$  are identical under both scenarios, however, the model fittings and the resulting  $K_p$  are different because of the differing patterns of hepatic enzyme zonation. The predicted liver concentrations mainly differ at early time points and are almost identical after 20 min post dosing (Figure 6). The SCM with lower  $ER/CL_{int}$  at the PP region (Scenario 1)

predicted higher  $T_{max}$ ,  $C_{max}$ , and  $AUC_{inf}$ , but a lower  $K_p$  value as compared to those predicted by the SCM with lower  $ER/CL_{int}$  at the PV region (Scenario 2). The model predictions and resulting parameters of the SCM with evenly distributed  $ER/CL_{int}$  lie in between those two testing scenarios (Figure 6 and Table 3). To achieve the same  $ER$ , the zonal SCM require a higher total  $CL_{int}$  (183.6 mL/min/kg) than the SCM with an even distribution of enzymatic activity throughout all the liver segments (151.2 mL/min/kg) (Table 3). Nevertheless, the model performance is comparable regardless of the hepatic heterogeneity of metabolic enzymes as suggested by the AIC values shown in Table 3.

The effects of enzyme zonation on the intrahepatic concentration gradients as a function of time and tissue space were assessed using the 5-compartment SCM and the data for DLZ. The  $C_{hi}$ -time profiles of DLZ predicted by the zonal SCM are presented in Figure 7a-c. For all models, the  $C_{max}$  of the subsequent compartment is always less than that of the previous one with the concentration-time curves shifting to the right as the drug moves from the PP region to the PV region and being metabolized. As compared to the case of evenly distributed metabolic clearance, the  $C_{max}$  of each liver sub-compartment decreases slower with a less delay in  $T_{max}$  when metabolism primarily occurs at the PV region (Scenario 1), while a faster drop in  $C_{max}$  and a more remarkable delay in  $T_{max}$  were observed when metabolic clearance mainly locates at the PP region (Scenario 2).

The predicted tissue ( $C_h$ ) and venous blood ( $C_{out}$ ) concentration gradients of DLZ from the inlet to the outlet of the liver at one time point after pseudo equilibrium (e.g., 180 min) are displayed in Figure 7d-f, where  $C_{out}$  was calculated from  $C_h$  and the estimated  $K_p$  values (Table 3) using Eq. 7 assuming  $R_b=1$ . As can be seen, different hepatic enzyme zonation results in differed intra-organ concentration gradients. Figure 7d shows a slow initial decrease in both  $C_h$  and  $C_{out}$  at the

PP region where the metabolic clearance was low so that the drug can accumulate before being exposed to the higher enzymatic activity at the PV region where a faster drop in both  $C_h$  and  $C_{out}$  was observed. When the metabolic clearance is evenly distributed, the drug is equally extracted (i.e., equal  $ER$ ,  $CL_{int}$  and  $F$ ) by all the liver sub-compartments so that  $C_h$  and  $C_{out}$  exhibit a constant rate of decline from the PP to the PV region (Figure 7e). In contrast, there is an immediate initial drop in both  $C_h$  and  $C_{out}$  when the PP region has higher intrinsic clearance and the decreases in both concentrations become less remarkable as the drug moves toward the PV region where the intrinsic clearance is low (Figure 7f).

As shown by Figure 7d-f, the zonal distribution of hepatic enzymes also has an impact on the tissue space-averaged blood concentration (red dashed lines), which is the highest (37.6 ng/mL) when metabolism was mainly at the PV region followed by that with an even distribution (22.7 ng/mL), and the lowest (13.2 ng/mL) when metabolism primarily occurs at the PP region.

The  $C_{out}$ -time profiles leaving the last liver segment predicted by the zonal SCM with  $n=2$  and 5 as a function of hepatic enzyme zonation are displayed in Figure 8. Regardless of the value of  $n$ , the SCM exhibiting lower metabolic clearance at the PV region (Scenario 2) yields a lower (2.3-fold decrease in  $C_{max}$ ) and later peak (3.1-fold increase in  $T_{max}$ ) of  $C_{out}$ -time profile than that obtained under Scenario 1 (i.e., lower metabolic clearance at the PP region), with the SCM of even enzyme distribution showing the intermediate profile. Consistent with those shown in Figure 5, a more significant delay in  $T_{max}$  is observed when there are more liver segments incorporated in the SCM given the same enzyme zonation. A 10-fold shallower gradient of metabolic clearances (i.e., when  $a=1.6$  or  $1/1.6$ ) has been tested, but a 2-fold difference was still observed in both  $C_{max}$  and  $T_{max}$  of the  $C_{out5}$ -time profiles (Table S2 and Figure S2). For drugs with a narrow therapeutic window or requiring a delayed or immediate onset of effects, a 2-3-

fold change in  $C_{max}$  or  $T_{max}$  may result in significant impacts on predicting drug efficacy and/or safety.

For the zonal SCM, the difference between hepatic availabilities in two adjacent liver segments ( $F_i$  and  $F_{(i+1)}$ ,  $F_{(i+1)} = F_i^a$ ) ( $i=1, \dots, n-1$ ) resulting from differed hepatic enzyme zonation also plays a role in the estimation of  $CL_{int}$  and  $K_p$  in PBPK. The changes in  $CL_{int}$  and  $K_p$  estimates with changing values of  $a$ , the exponential of  $F_i$  ( $i=1, \dots, n-1$ ), were examined and presented in Figure 9. All model fittings were performed assuming lower metabolic clearances at the PP region with the  $ER$  of DLZ remaining unchanged. As indicated in Figure 9a, the estimated total  $CL_{int}$  of the zonal SCM lies in between those of the two extreme cases (viz. WSM and PTM) regardless of the changes in the number of liver sub-compartments ( $n$ ) and the exponential of  $F_i$  ( $a$ ), consistent with the previous demonstrations (Figure 2). The total  $CL_{int}$  of the zonal SCM decreases with increasing  $n$  but increases and approaches the WSM-estimated intrinsic clearance ( $CL_{int, WSM}$ ) as the difference between the metabolic clearance in two adjacent liver segments becomes larger. The estimated  $K_p$  show the same dependency on  $n$  as  $CL_{int}$ , i.e., the SCM with a larger  $n$  produces a smaller  $K_p$  given the same zonation of hepatic enzymes. However, in contrast to the relationship between  $CL_{int}$  and  $a$ , the estimated  $K_p$  is negatively correlated with  $a$  and becomes less than that obtained by the PTM ( $K_{p, PTM}$ ) as  $a$  increases (Figure 9b).

## Discussion

In PBPK modeling, the true  $CL_{int}$  and  $K_p$  are an ‘unknowable’ mystery in the ‘black box’ of the liver and the differential equations that describe total liver concentrations require an assumed model with these parameters that are model-dependent (Li and Jusko, 2022). The SCM offers an alternative to the WSM, PTM, and DM with close resemblance to the latter and offering many flexibilities to better approximate the known or expected functioning and concentrations in the liver.

The SCM was initially used to describe the dilution curves of non-eliminating tracers from organs where the flow through a blood vessel was modeled as a series of identical well-stirred chambers with the same volumes (Davenport, 1983). Our studies confirm the SCM as an alternative to the complex DM as they share some mathematical similarities (Goresky et al., 1973; Roberts and Rowland, 1986a; Gray and Tam, 1987) with fewer computation complexities and offering advantages in describing a variety of phenomena including PBPK profiles. It was not clear from prior work how closely the SCM and DM are quantitatively related. The major determinants differentiating the SCM and DM from the WSM and PTM, the two limiting cases of the basic hepatic clearance models, are the number of liver sub-compartments ( $n$ ) and the dispersion number ( $D_N$ ). In this work, the values of  $n$  and  $D_N$  were found to play a dominant role in comparing the SCM and DM. The changes in  $ER$  vs  $CL_{int}$  profiles of the SCM with increasing  $n$  exhibit the same trend as those of the DM with decreasing  $D_N$ ; specifically the SCM with  $n = 2$  and 5 yield almost identical  $ER$  as those predicted by the DM with  $D_N = 0.6$  and 0.1, the boundary values of the  $D_N$  range (Obach et al., 1997; Oliver et al., 2001; Pang et al., 2019) given the same  $CL_{int}$  (Figure 2).

The SCM has had limited use as a model of hepatic elimination in PBPK. So far, such applications have mainly focused on the complex transporter SCM with  $n = 5$  (Watanabe et al., 2009; Jones et al., 2012; Morse et al., 2017) and it was unclear how changing  $n$  had an impact on the liver concentration-time data. In the 5-segment transporter SCM, at least four clearance terms (i.e., active uptake and biliary efflux, passive diffusion, and metabolic clearance) are involved, causing parameter identifiability issues (biliary and metabolic clearances cannot be uniquely identified through model-fitting). Many assumptions are required and substrate- and transporter-dependent empirical scaling factors (SF) are needed, especially for IVIVE. To assess the impact of  $n$  on the model performance of SCM in PBPK without either these or other complexities, the *in vivo* time course data of 6 flow-limited substances were examined. Interestingly, the model-dependencies in the estimated  $CL_{int}$  and PBPK-operative  $K_p$  as a function of  $n$  were shown to be the same, i.e., SCM ( $n=1$ ) (WSM)>SCM ( $n=2$ )>SCM ( $n=5$ )>PTM, indicating that the assumed average unbound tissue/blood concentrations within the liver for the SCM are lower when  $n$  is smaller given the same  $ER$ . These findings are similar to our recent analysis where the rank order of  $CL_{int}$  and  $K_p$  was WSM>DM ( $D_N=0.6$ )>PTM (Li and Jusko, 2022). In model fittings, the choice of  $n$  mainly affects the prediction of early total liver concentrations as reflected by the higher  $C_{max}$  (all compounds) and delayed  $T_{max}$  (FTY720, VEM and DLZ) with larger values of  $n$  although minor differences in  $AUC_{inf}$  were observed. Such differences in model fittings suggest that the optimal  $n$  value of the SCM may not be readily identifiable by merely fitting *in vivo* time course data if early observations are missing, especially when lacking IV data.

Hepatic zonal heterogeneity of key metabolizing enzymes and its potential effects on hepatic metabolism of xenobiotics are known (Jungermann, 1986; Gebhardt, 1992; Tirona and Pang, 1996; Oinonen and Lindros, 1998; Cunningham and Porat-Shliom, 2021). For instance, the

expression of major drug-metabolizing cytochrome P-450 enzymes (CYP450s) is higher in the downstream PV region of the liver than in the PP region, with a 30 to 60-fold difference reported for CYP2E1 (Buhler et al., 1992; Tachikawa et al., 2018). Among the phase II reactions, glucuronidation occurs preferentially in the PV cells, and sulphation is greater in the PP cells (Jungermann and Katz, 1989; Jungermann, 1995). Traditional hepatic clearance models assume uniform distribution of metabolic enzymes in the liver, which does not represent the true physiology. The SCM allows for hepatic enzyme zonation by assigning different  $CL_{int}$  values to each liver segment. For example, a 3-zone SCM (i.e., PP-, mid-, and PV-zone) with differing metabolic clearances (i.e., PV/PP esterase activity = 6.6) obtained by examining the metabolic activities toward enalapril in S9 fractions of enriched rat PP and PV hepatocytes was applied to characterize the uneven ester hydrolysis of enalapril in rat liver based on *in vitro* and perfusion data (Abu-Zahra and Pang, 2000). The effect of zonal differences in metabolism on the translation of  $K_{pu}$  from *in vitro* to *in vivo* was explored theoretically using a 5-segment model where a 256-fold difference in metabolic clearances between the PP and PV regions was assigned (Li et al., 2019). However, none of these assessments were based on assessing *in vivo* PBPK-type time course data. By assigning liver segment-specific  $CL_{int}$  values, we show that hepatic enzyme zonation produces more remarkable differences in the predicted total liver concentrations (Figure 6) as compared to the effects of  $n$  (Figure 3). It is worth noting that even with the same total  $CL_{int}$ , the model predictions and estimated  $K_p$  can differ depending on how the metabolic clearances are distributed as do the internal concentration gradients as a function of time and tissue space (Figure 7). The SCM with a lower  $CL_{int}$  at the PP region predicts the highest tissue space-averaged blood concentration (red dashed lines in Figure 7b); therefore, the tissue-to-plasma ratio is the smallest at the pseudo-equilibrium state given the comparable tissue



space-averaged liver concentrations (black dashed lines in Figure 7b) compared to the other models, consistent with the rank order of the estimated  $K_p$  based on the full curves (Table 3). Additionally, the estimation of total  $CL_{int}$  and  $K_p$  by the zonal SCM was also affected by the steepness of the metabolic clearance gradients within the liver as reflected by the value of  $a$  ( $F_{(i+1)} = F_i^a$ ,  $i=1, \dots, n-1$ ) (Figure 9). Similarly, hepatic transporters also exhibit zonal heterogeneity (Tachikawa et al., 2018), which may be included in the SCM if relevant information is available.

The hepatic WSM is often operated with PBPK modeling for IVIVE and to assess and predict Drug-Drug Interactions (DDIs). Such modeling with use of *in silico* tissue  $K_p$  values, when first optimized based on adjustments to capture known human plasma concentration versus time profiles (“top-down” or “middle-out”) is about 80% successful in predicting DDI AUC values within 1.25-fold. An IVIVE approach (“bottom-up”) is used infrequently (Wagner et al., 2015) and requires a large scaling factor when employed *de novo* for predicting hepatic clearance based on *in vitro*  $CL_{int}$  values (Tess et al., 2022). The SCM offers the possibility of application of a more flexible modeling approach for handling known complexities of the liver such as transporters and zonal differences in metabolism. The application of SCM in PBPK may also have important pharmacological/toxicological implications. For example, oral dosing with rapid absorption may exacerbate the differences in early model predictions as the initial concentration in the 1<sup>st</sup> liver sub-compartment ( $Dose/V_{hl}$ ) will be higher compared to that of an IV dose that undergoes tissue distribution. This is relevant when a drug shows hepatic toxicity. In addition to zonal expression, the regulation of hepatic enzymes also exhibits zonal dependency and was shown to be partially responsible for the zonal pattern of certain liver injuries (Wojcik et al., 1988; Buhler et al., 1992; Lindros, 1997; Oinonen and Lindros, 1998; McEnerney et al., 2017).

For instance, the regiospecific expression and induction of CYP2E1 play a major role in explaining the centrilobular damage caused by a high dose of acetaminophen (Anundi et al., 1993). This is worth consideration when assessing DDIs especially if liver is the target of efficacy or toxicity. When the systemic PK/exposure of the victim drug is not significantly affected by a perpetrator drug, it is possible that the concentrations of the victim drug at a certain zonal region of the liver might change significantly due to such position-dependent regulation and thereby result in suboptimal efficacy or potential local cell injury. Also, the predicted intrahepatic concentration gradient for the SCM differs appreciably with the value of  $n$ , which may have an impact when assessing PK/pharmacodynamic (PD) relationships if the assumed hepatic concentrations relate to the pharmacological effects and/or toxicity. All these aspects may be better assessed with the SCM as it allows incorporation of zonal expression and regulation of metabolic enzymes/transporters and the prediction of concentrations in each of the liver sub-compartments. The intra-organ concentration gradients are also expected to exist in other eliminating tissues, indicating a potential wider application of the SCM in addition to describing hepatic disposition. The SCM shares similar construction as transit compartment models where a series of compartments are connected by first-order processes in a catenary manner and described with serial differential equations (Sun and Jusko, 1998). Such models have been extensively utilized in accounting for various short to long time delays in PK and PK/ PD when information is lacking about the intermediary steps causing delays. Such applications include delayed drug absorption and biliary excretion (Bischoff et al., 1971; Savic et al., 2007; Kagan et al., 2010; Lachi-Silva et al., 2015), drug movement along the spinal cord (Heetla et al., 2016), delayed pharmacological responses due to signal transduction processes (Byun et al., 2022), and for disease progression modeling (Earp et al., 2008). There is considerable flexibility

and variety in the number of transit steps and the time constants. This is partly similar for hepatic SCM models, although the physiologic volume/flow rates control the time constants (Eq. 9). The intra-organ concentrations decrease down the compartments in a stepwise fashion (Figure 4). As a result, an SCM with more liver segments produces greater delays in the time profiles of outflow blood concentrations from the last liver segment ( $C_{outn}$ ) (Figure 5). On top of this, a higher  $CL_{int}$  at the PP region predicts even further delayed  $C_{outn}$ -time profiles especially with larger values of  $n$  (Figure 8). As  $C_{outn}$  enters the venous blood pool, such differences may have an impact on the kinetics in other tissues in full PBPK analyses. Furthermore, if the SCM is paired with the wrong  $K_p$  for simulation purposes, it could appreciably distort capturing the liver concentrations as shown in Figure S3. One of the limitations of this study is that the gradient of intrinsic clearances existing between the PP and PV regions was arbitrarily assigned by setting  $a$  value to 2 and 0.5 (i.e., about 100-fold difference in the gradient of metabolic activity). This may not be true for the compounds assessed herein, however, it should suffice for examining the trends of changes in model fittings and parameter estimates (e.g.,  $CL_{int}$  and  $K_p$ ) resulting from the metabolic zonation as compared to even enzyme distribution that has been commonly assumed and applied.

In this work, the quantitative equivalency between the SCM and DM was demonstrated through theoretical simulations and fittings of plasma/liver data by PBPK modeling, and factors that need to be considered when applying the SCM were proposed. As was shown, 5 sub-compartments seem to be sufficient for the SCM to mimic the DM and will have to be accepted as reasonable. Without extremely frequent early liver data, the best  $n$ -SCM cannot be ascertained. Despite of certain limitations, zone-specific intrinsic clearances may be obtained using isolated hepatocytes from various regions of the liver (Abu-Zahra and Pang, 2000) as a starting point for constructing

more physiologically-based zonal SCM for IVIVE. With advances in technology, it may be possible to collect samples from different zonal regions of the liver to validate the predicted concentrations in liver sub-compartments by the SCM and further aid model selection and refinements. In conclusion, the model-dependencies in the predicted total/intrahepatic concentrations and the estimates of  $CL_{int}$  and PBPK-operative  $K_p$  as a function of  $n$  and hepatic enzyme zonation are most relevant when: 1) the SCM is used for IVIVE in that a model-dependent  $ER$  will be expected from the same *in vitro*  $CL_{int}$ , 2) different SCM are applied with  $K_p$  from the same source (such as *in silico* predictions) in PBPK that will likely yield different liver predictions, 3) assessing PK/PD/toxicity relationships if the assumed hepatic concentrations are the driving forces. Besides those factors assessed herein, other complexities such as transporter heterogeneity and nonlinear  $CL_{int}$  or  $K_p$  may be further added to the SCM given suitable experimental information.

## **Authorship Contributions**

*Participated in research design:* Li and Jusko.

*Performed data analysis:* Li.

*Wrote or contributed to the writing of the manuscript:* Li and Jusko.

## References

- Abu-Zahra TN and Pang KS (2000) Effect of zonal transport and metabolism on hepatic removal: enalapril hydrolysis in zonal, isolated rat hepatocytes in vitro and correlation with perfusion data. *Drug Metab Dispos* **28**:807-813.
- Anundi I, Lahteenmaki T, Rundgren M, Moldeus P, and Lindros KO (1993) Zonation of acetaminophen metabolism and cytochrome P450 2E1-mediated toxicity studied in isolated periportal and perivenous hepatocytes. *Biochem Pharmacol* **45**:1251-1259.
- Bischoff KB, Dedrick RL, Zaharko DS, and Longstreth JA (1971) Methotrexate pharmacokinetics. *J Pharm Sci* **60**:1128-1133.
- Brown RP, Delp MD, Lindstedt SL, Rhombert LR, and Beliles RP (1997) Physiological parameter values for physiologically based pharmacokinetic models. *Toxicol Ind Health* **13**:407-484.
- Buffham BA and Gibilaro L (1968) A generalization of the tanks-in-series mixing model. *AIChE J* **14**:805-806.
- Buhler R, Lindros KO, Nordling A, Johansson I, and Ingelman-Sundberg M (1992) Zonation of cytochrome P450 isozyme expression and induction in rat liver. *Eur J Biochem* **204**:407-412.
- Byun JH, Yoon IS, Lee SY, Cho HJ, and Jung IH (2022) Extended transit compartment model to describe tumor delay using Coxian distribution. *Sci Rep* **12**:10086.
- Cheung SYA, Rodgers T, Aarons L, Gueorguieva I, Dickinson GL, Murby S, Brown C, Collins B, and Rowland M (2018) Whole body physiologically based modelling of beta-blockers in the rat: events in tissues and plasma following an i.v. bolus dose. *Br J Pharmacol* **175**:67-83.
- Chou CH, Evans AM, Fornasini G, and Rowland M (1993) Relationship between lipophilicity and hepatic dispersion and distribution for a homologous series of barbiturates in the isolated perfused in situ rat liver. *Drug Metab Dispos* **21**:933-938.
- Cunningham RP and Porat-Shliom N (2021) Liver Zonation - Revisiting Old Questions With New Technologies. *Front Physiol* **12**:732929.
- D'Argenio D, Schumitzky A, and Wang X (2009) *Adapt 5 User's Guide: Pharmacokinetic/Pharmacodynamic Systems Analysis Software*. BMSR, University of Southern California.
- Davenport R (1983) The derivation of the gamma-variate relationship for tracer dilution curves. *J Nucl Med* **24**:945-948.
- Diaz-Garcia JM, Evans AM, and Rowland M (1992) Application of the axial dispersion model of hepatic drug elimination to the kinetics of diazepam in the isolated perfused rat liver. *J Pharmacokinet Biopharm* **20**:171-193.
- Earp JC, Dubois DC, Molano DS, Pyszczyński NA, Keller CE, Almon RR, and Jusko WJ (2008) Modeling corticosteroid effects in a rat model of rheumatoid arthritis I: mechanistic disease progression model for the time course of collagen-induced arthritis in Lewis rats. *J Pharmacol Exp Ther* **326**:532-545.
- Ebling WF, Wada DR, and Stanski DR (1994) From piecewise to full physiologic pharmacokinetic modeling: Applied to thiopental disposition in the rat. *J Pharmacokinet Biopharm* **22**:259-292.

- Evans AM, Hussein Z, and Rowland M (1993) Influence of albumin on the distribution and elimination kinetics of diclofenac in the isolated perfused rat liver: Analysis by the impulse-response technique and the dispersion model. *J Pharm Sci* **82**:421-428.
- Foster DM (1998) Developing and testing integrated multicompartment models to describe a single-input multiple-output study using the SAAM II software system. *Adv Exp Med Biol* **445**:59-78.
- Gebhardt R (1992) Metabolic zonation of the liver: regulation and implications for liver function. *Pharmacol Ther* **53**:275-354.
- Goresky CA, Bach GG, and Nadeau BE (1973) On the uptake of materials by the intact liver. The transport and net removal of galactose. *J Clin Invest* **52**:991-1009.
- Gray MR and Tam YK (1987) The series-compartment model for hepatic elimination. *Drug Metab Dispos* **15**:27-31.
- Gueorguieva I, Nestorov IA, Murby S, Gisbert S, Collins B, Dickens K, Duffy J, Hussain Z, and Rowland M (2004) Development of a whole body physiologically based model to characterise the pharmacokinetics of benzodiazepines. 1: Estimation of rat tissue-plasma partition ratios. *J Pharmacokinet Pharmacodyn* **31**:269-298.
- Hallifax D, Foster JA, and Houston JB (2010) Prediction of human metabolic clearance from in vitro systems: Retrospective analysis and prospective view. *Pharm Res* **27**:2150-2161.
- Heetla HW, Proost JH, Molmans BH, Staal MJ, and van Laar T (2016) A pharmacokinetic-pharmacodynamic model for intrathecal baclofen in patients with severe spasticity. *Br J Clin Pharmacol* **81**:101-112.
- Houston JB (1994) Utility of in vitro drug metabolism data in predicting in vivo metabolic clearance. *Biochem Pharmacol* **47**:1469-1479.
- Igari Y, Sugiyama Y, Sawada Y, Iga T, and Hanano M (1983) Prediction of diazepam disposition in the rat and man by a physiologically based pharmacokinetic model. *J Pharmacokinet Biopharm* **11**:577-593.
- Jones HM, Barton HA, Lai Y, Bi YA, Kimoto E, Kempshall S, Tate SC, El-Kattan A, Houston JB, Galetin A, and Fenner KS (2012) Mechanistic pharmacokinetic modeling for the prediction of transporter-mediated disposition in humans from sandwich culture human hepatocyte data. *Drug Metab Dispos* **40**:1007-1017.
- Jungermann K (1986) Functional heterogeneity of periportal and perivenous hepatocytes. *Enzyme* **35**:161-180.
- Jungermann K (1995) Zonation of metabolism and gene expression in liver. *Histochem Cell Biol* **103**:81-91.
- Jungermann K and Katz N (1989) Functional specialization of different hepatocyte populations. *Physiol Rev* **69**:708-764.
- Jusko WJ and Li X (2021) Assessment of the Kochak-Benet equation for hepatic clearance for the parallel-tube model: Relevance of classic clearance concepts in PK and PBPK. *AAPS J* **24**:5.
- Kagan L, Dreifinger T, Mager DE, and Hoffman A (2010) Role of p-glycoprotein in region-specific gastrointestinal absorption of talinolol in rats. *Drug Metab Dispos* **38**:1560-1566.
- Kashiwagi T, Kimura K, Suematsu T, Schichiri M, Kamada T, and Abe H (1981) Heterogeneous intrahepatic distribution of blood flow in humans. *Eur J Nucl Med* **6**:545-549.
- Kawai R, Mathew D, Tanaka C, and Rowland M (1998) Physiologically based pharmacokinetics of cyclosporine A: Extension to tissue distribution kinetics in rats and scale-up to human. *J Pharmacol Exp Ther* **287**:457-468.

- Lachi-Silva L, Sy SK, Voelkner A, de Sousa JP, Lopes JL, Silva DB, Lopes NP, Kimura E, Derendorf H, and Diniz A (2015) Simultaneous characterization of intravenous and oral pharmacokinetics of lychnopholide in rats by transit compartment model. *Planta Med* **81**:1121-1127.
- Lee JB, Zhou S, Chiang M, Zang X, Kim TH, and Kagan L (2020) Interspecies prediction of pharmacokinetics and tissue distribution of doxorubicin by physiologically-based pharmacokinetic modeling. *Biopharm Drug Dispos* **41**:192-205.
- Levenspiel O (1999) *Chemical Reaction Engineering*. John Wiley & Sons.
- Li R, Barton HA, Yates PD, Ghosh A, Wolford AC, Riccardi KA, and Maurer TS (2014) A "middle-out" approach to human pharmacokinetic predictions for OATP substrates using physiologically-based pharmacokinetic modeling. *J Pharmacokinet Pharmacodyn* **41**:197-209.
- Li R, Maurer TS, Sweeney K, and Barton HA (2016) Does the systemic plasma profile inform the liver profile? Analysis using a physiologically based pharmacokinetic model and individual compounds. *AAPS J* **18**:746-756.
- Li X and Jusko WJ (2022) Assessing liver-to-plasma partition coefficients and in silico calculation methods: when does the hepatic model matter in PBPK? *Drug Metab Dispos*.
- Li Z, Di L, and Maurer TS (2019) Theoretical considerations for direct translation of unbound liver-to-plasma partition coefficient from in vitro to in vivo. *AAPS J* **21**:43.
- Lin JH, Hayashi M, Awazu S, and Hanano M (1978) Correlation between in vitro and in vivo drug metabolism rate: oxidation of ethoxybenzamide in rat. *J Pharmacokinet Biopharm* **6**:327-337.
- Lindros KO (1997) Zonation of cytochrome P450 expression, drug metabolism and toxicity in liver. *Gen Pharmacol* **28**:191-196.
- McEnerney L, Duncan K, Bang BR, Elmasry S, Li M, Miki T, Ramakrishnan SK, Shah YM, and Saito T (2017) Dual modulation of human hepatic zonation via canonical and non-canonical Wnt pathways. *Exp Mol Med* **49**:e413.
- Meno-Tetang GM, Li H, Mis S, Pyszczynski N, Heining P, Lowe P, and Jusko WJ (2006) Physiologically based pharmacokinetic modeling of FTY720 (2-amino-2[2-(4-octylphenyl)ethyl]propane-1,3-diol hydrochloride) in rats after oral and intravenous doses. *Drug Metab Dispos* **34**:1480-1487.
- Miller NA, Reddy MB, Heikkinen AT, Lukacova V, and Parrott N (2019) Physiologically based pharmacokinetic modelling for first-in-human predictions: An updated model building strategy illustrated with challenging industry case studies. *Clin Pharmacokinet* **58**:727-746.
- Morse BL, MacGuire JG, Marino AM, Zhao Y, Fox M, Zhang Y, Shen H, Griffith Humphreys W, Marathe P, and Lai Y (2017) Physiologically based pharmacokinetic modeling of transporter-mediated hepatic clearance and liver partitioning of OATP and OCT substrates in cynomolgus monkeys. *AAPS J* **19**:1878-1889.
- Obach RS, Baxter JG, Liston TE, Silber BM, Jones BC, MacIntyre F, Rance DJ, and Wastall P (1997) The prediction of human pharmacokinetic parameters from preclinical and in vitro metabolism data. *J Pharmacol Exp Ther* **283**:46-58.
- Oinonen T and Lindros KO (1998) Zonation of hepatic cytochrome P-450 expression and regulation. *Biochem J* **329** ( Pt 1):17-35.



- Oliver RE (1995) Development of a whole-body physiological model based on dispersion concepts to describe the pharmacokinetics of drug in the body, in: *Department of Pharmacy*, pp 246, University of Manchester, Manchester, UK.
- Oliver RE, Jones AF, and Rowland M (2001) A whole-body physiologically based pharmacokinetic model incorporating dispersion concepts: short and long time characteristics. *J Pharmacokinet Pharmacodyn* **28**:27-55.
- Pang KS, Han YR, Noh K, Lee PI, and Rowland M (2019) Hepatic clearance concepts and misconceptions: Why the well-stirred model is still used even though it is not physiologic reality? *Biochem Pharmacol* **169**:113596.
- Pang KS and Rowland M (1977) Hepatic clearance of drugs. I. Theoretical considerations of a "well-stirred" model and a "parallel tube" model. Influence of hepatic blood flow, plasma and blood cell binding, and the hepatocellular enzymatic activity on hepatic drug clearance. *J Pharmacokinet Biopharm* **5**:625-653.
- Rane A, Wilkinson GR, and Shand DG (1977) Prediction of hepatic extraction ratio from in vitro measurement of intrinsic clearance. *J Pharmacol Exp Ther* **200**:420-424.
- Roberts MS and Rowland M (1986a) A dispersion model of hepatic elimination: 1. Formulation of the model and bolus considerations. *J Pharmacokinet Biopharm* **14**:227-260.
- Roberts MS and Rowland M (1986b) A dispersion model of hepatic elimination: 2. Steady-state considerations--influence of hepatic blood flow, binding within blood, and hepatocellular enzyme activity. *J Pharmacokinet Biopharm* **14**:261-288.
- Rowland M, Benet LZ, and Graham GG (1973) Clearance concepts in pharmacokinetics. *J Pharmacokinet Biopharm* **1**:123-136.
- Savic RM, Jonker DM, Kerbusch T, and Karlsson MO (2007) Implementation of a transit compartment model for describing drug absorption in pharmacokinetic studies. *J Pharmacokinet Pharmacodyn* **34**:711-726.
- Sun YN and Jusko WJ (1998) Transit compartments versus gamma distribution function to model signal transduction processes in pharmacodynamics. *J Pharm Sci* **87**:732-737.
- Tachikawa M, Sumiyoshiya Y, Saigusa D, Sasaki K, Watanabe M, Uchida Y, and Terasaki T (2018) Liver Zonation Index of Drug Transporter and Metabolizing Enzyme Protein Expressions in Mouse Liver Acinus. *Drug Metab Dispos* **46**:610-618.
- Tess DA, Ryu S, and Di L (2022) In Vitro - in Vivo Extrapolation of Hepatic Clearance in Preclinical Species. *Pharm Res* **39**:1615-1632.
- Tirona RG and Pang KS (1996) Sequestered endoplasmic reticulum space for sequential metabolism of salicylamide. Coupling of hydroxylation and glucuronidation. *Drug Metab Dispos* **24**:821-833.
- Tomlinson L, Hyndman L, Firman JW, Bentley R, Kyffin JA, Webb SD, McGinty S, and Sharma P (2019) In vitro liver zonation of primary rat hepatocytes. *Front Bioeng Biotechnol* **7**:17.
- Wagner C, Pan Y, Hsu V, Grillo JA, Zhang L, Reynolds KS, Sinha V, and Zhao P (2015) Predicting the effect of cytochrome P450 inhibitors on substrate drugs: analysis of physiologically based pharmacokinetic modeling submissions to the US Food and Drug Administration. *Clin Pharmacokinet* **54**:117-127.
- Watanabe T, Kusuhara H, Maeda K, Shitara Y, and Sugiyama Y (2009) Physiologically based pharmacokinetic modeling to predict transporter-mediated clearance and distribution of pravastatin in humans. *J Pharmacol Exp Ther* **328**:652-662.

- Wojcik E, Dvorak C, Chianale J, Traber PG, Keren D, and Gumucio JJ (1988) Demonstration by in situ hybridization of the zonal modulation of rat liver cytochrome P-450b and P-450e gene expression after phenobarbital. *J Clin Invest* **82**:658-666.
- Yamano K, Yamamoto K, Kotaki H, Takedomi S, Matsuo H, Sawada Y, and Iga T (2000) Quantitative prediction of metabolic inhibition of midazolam by erythromycin, diltiazem, and verapamil in rats: implication of concentrative uptake of inhibitors into liver. *J Pharmacol Exp Ther* **292**:1118-1126.

## Footnotes

This work was supported by NIH Grant R35 GM131800. No author has an actual or perceived conflict of interest with the contents of this article.

## Figure Legends

**Figure 1.** Schematic diagram of the series-compartment model of hepatic elimination, where  $Q_h$  is hepatic blood flow,  $C$  are indicated drug concentrations,  $V_{hi}$  are volumes of sub-compartments, and  $CL_{int,i}$  is intrinsic clearance.

**Figure 2.** Relationships between Extraction Ratio ( $ER$ ) and  $CL_{int}$  of the SCM and indicated basic hepatic clearance models.

**Figure 3.** Blood and liver concentration-time profiles of 6 selected compounds listed in Table 1. The circles show the observed blood (red) and liver (black) concentrations. The colored solid lines indicate the model fittings of the blood data (red), and the liver data by the SCM with  $n=1$  (purple),  $n=2$  (orange), and  $n=5$  (green). The inset graphs show the liver concentration-time profiles at early time points for better visualization of differences in the model predictions.

**Figure 4.** Predicted liver concentration ( $C_{hi}$ ,  $i=1, 2...5$ )-time profiles of the selected compounds in each of the sub-compartments by the SCM containing 2 (2CM) and 5 (5CM) liver segments. Customized time scales were applied to better visualize the differences.

**Figure 5.** Diltiazem (DLZ) concentration-time profiles in the venous blood leaving the last liver sub-compartment ( $C_{outn}$ ,  $n=1, 2$ , and  $5$ ) predicted by the SCM containing 1, 2 and 5 liver segments.

**Figure 6.** Blood and liver concentration-time profiles of DLZ. Measured concentrations in blood (red) and liver (black) are indicated by symbols. Solid lines show the model fittings of the blood (red) and liver data by the SCM with lower  $ER/CL_{int}$  at the PP region (Scenario 1, purple), equal distribution of  $ER/CL_{int}$  (green), and lower  $ER/CL_{int}$  at the PV region (Scenario 2, orange). The estimated total  $f_{ub}CL_{int}$  and  $K_p$  values are listed for each of the models with the same color coding as those for the liver model fittings.

**Figure 7.** Hepatic  $C_{hi}$ -time profiles (panels a-c) and 180-min  $C_h$  (black solid circles) and  $C_{out}$  (red solid circles) (panels d-f) of DLZ in liver sub-compartment  $i$  ( $i=1, 2, \dots, 5$ ) predicted by the SCM with lower metabolic clearance at the PP region (Scenario 1, panels a and d), even distribution of metabolic clearance (panels b and e), and lower metabolic clearance at the PV region (Scenario 2, panels c and f). In panels d-f, the dashed lines represent the tissue-space averaged  $C_h$  (black) and  $C_{out}$  (red) of the whole liver tissue, the open bars indicate the estimated  $f_{ub}CL_{int}$  in liver sub-compartment  $i$  ( $i=1, 2, \dots, 5$ ), and the black arrows represent the direction from the inlet to the outlet of the liver.

**Figure 8.** Outflow blood concentration-time profiles of DLZ from the last liver sub-compartment of the SCM as a function of  $n$  and hepatic enzyme zonation.

**Figure 9.** Changes in the estimated total  $CL_{int}$  (a) and  $K_p$  (b) of DLZ by the zonal SCM as a function of  $n$  and  $a$  ( $F_{(i+1)} = F_i^a$ ,  $i=1 \dots n-1$ ). Colored dashed lines indicate the total  $CL_{int}$  and  $K_p$  of DLZ estimated by the WSM (purple) and PTM (blue).

Table 1. Parameters estimated from the blood/liver concentration-time profiles <sup>a</sup> of indicated compounds by the SCM of differed *n*

Compound	<i>ER</i>	SCM	Estimates (CV%)				AIC
			<i>CL<sub>b</sub></i> <sup>b</sup>	<i>ER</i> <sup>b</sup>	<i>f<sub>ub</sub>CL<sub>int</sub></i> <sup>c</sup>	<i>K<sub>p</sub></i>	
Cyclosporine (CyA)	0.06	<i>n</i> =1			3.79 (1.7)	16.56 (14.8)	74.7
		<i>n</i> =2	2.77	0.06 (1.6)	3.73 (1.7)	16.35 (14.5)	74.3
		<i>n</i> =5			3.70 (1.7)	16.36 (14.2)	73.9
Ethoxybenzamide (EB)	0.08	<i>n</i> =1			5.55 (4.9)	1.25 (9.7)	44.9
		<i>n</i> =2	4.92	0.08 (6.3)	5.43 (4.8)	1.22 (9.5)	44.8
		<i>n</i> =5			5.36 (4.8)	1.22 (9.0)	41.6
Fingolimod (FTY720)	0.17	<i>n</i> =1			12.21 (8.5)	61.86 (9.3)	205.5
		<i>n</i> =2	7.89	0.17 (7.1)	11.66 (8.1)	59.58 (9.6)	205.9
		<i>n</i> =5			11.34 (7.9)	57.95 (9.5)	206.4
Diazepam (DZP)	0.66	<i>n</i> =1			118.1 (16.9)	10.54 (20)	128
		<i>n</i> =2	38.8	0.66 (5.7)	86.99 (13.4)	8.26 (20.4)	129
		<i>n</i> =5			73.24 (11.5)	7.16 (23.4)	130

Verapamil (VEM)	0.7	$n=1$			145.0 (4.6)	25.05 (5.5)	175
		$n=2$	42.8	0.7 (1.4)	102.1 (3.6)	17.68 (5.9)	176
		$n=5$			83.93 (3)	14.60 (6.2)	178
Diltiazem (DLZ)	0.87	$n=1$			396.6 (15.7)	26.30 (7.1)	158
		$n=2$	52.7	0.87 (2.1)	211.9 (10.7)	14.11 (7.2)	158
		$n=5$			151.2 (8.2)	10.11 (7.3)	159

<sup>a</sup> Literature sources for the modeling datasets are (Kawai et al., 1998) for CyA, (Lin et al., 1978) for EB, (Igari et al., 1983) for DZP, (Meno-Tetang et al., 2006) for FTY720, and (Yamano et al., 2000) for VEM and DLZ.

<sup>b</sup>  $CL_b$  and  $ER$  were calculated based on Eq. 17-18 using the reported  $Q_h$  in the source literature of the modeling datasets except for VEM and DLZ for which the  $Q_h$  value of 60.82 mL/min/kg (Brown et al., 1997) was used since it was not reported in (Yamano et al., 2000); The  $CL_b$  have the same CV% values as those of estimated  $ER$ .

<sup>c</sup> With the estimated  $ER$ ,  $f_{ub}CL_{int}$  for the SCM of different  $n$  were calculated using the  $Q_h$  of 60.82 mL/min/kg (Brown et al., 1997) according to Eq. 2-5.

Table 2. Changes in  $C_{max}$ ,  $T_{max}$  and  $AUC_{inf}$  of the predicted total liver concentrations by the SCM as a function of  $n$  (percentage of those predicted by the SCM with  $n = 1$ )

Compound	ER	SCM	$C_{max}$	$T_{max}$	$AUC_{inf}$
CyA	0.06	$n=1$	100	100	100
		$n=2$	117	100	100
		$n=5$	135	100	101
EB	0.08	$n=1$	100	100	100
		$n=2$	114	100	100
		$n=5$	130	92	101
FTY720	0.17	$n=1$	100	100	100
		$n=2$	112	100	101
		$n=5$	120	200	101
DZP	0.66	$n=1$	100	100	100
		$n=2$	110	100	107
		$n=5$	118	100	109
VEM	0.7	$n=1$	100	100	100



		<i>n</i> =2	104	109	100
		<i>n</i> =5	106	118	101
		<i>n</i> =1	100	100	100
DLZ	0.87	<i>n</i> =2	103	100	100
		<i>n</i> =5	104	112	101

Table 3. Parameters obtained from fitting the liver data of DLZ by the SCM with zonal and even distribution of hepatic enzymes

Parameter (Unit)	Estimates (CV%)		
	Scenario 1	Scenario 2	Even Distribution
	(Lower PP $ER/CL_{int}$ )	(Lower PV $ER/CL_{int}$ )	(Equal $ER/CL_{int}$ )
$f_{ub}CL_{int1}$ (mL/min/kg) <sup>a</sup>	4.09	111.47	
$f_{ub}CL_{int2}$ (mL/min/kg) <sup>a</sup>	8.45	41.54	
$f_{ub}CL_{int3}$ (mL/min/kg) <sup>a</sup>	18.08	18.08	30.24 <sup>b</sup>
$f_{ub}CL_{int4}$ (mL/min/kg) <sup>a</sup>	41.54	8.45	
$f_{ub}CL_{int5}$ (mL/min/kg) <sup>a</sup>	111.47	4.09	
$f_{ub}CL_{int}$ (mL/min/kg) <sup>a</sup>	183.64		151.2 (8.2)
$K_p$	6.16 (7.03)	17.09 (6.52)	10.11 (7.3)
$T_{max}$ (min)	1.21	0.85	1.09
$C_{max}$ (ng/mL)	40387	28005	34339
$AUC_{inf}$ (ng*hr/mL)	363932	347483	358774
AIC	158.7	156.2	159

<sup>a</sup>  $f_{ub}CL_{inti}$  ( $i=1,2,...5$ ) was calculated from  $ER$  of DLZ using Eq. 3-4, 20-23 and fixed in the model fitting of liver data;  $f_{ub}CL_{int}$  is the sum of  $f_{ub}CL_{inti}$  of all liver compartments.

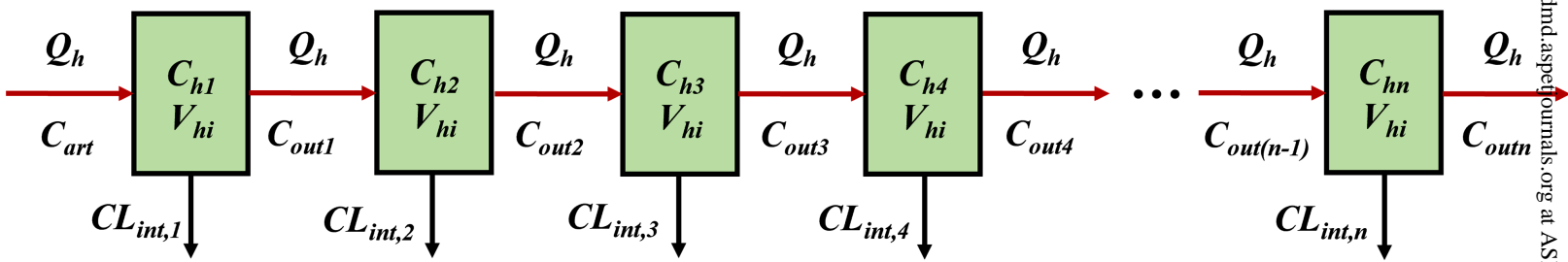


**Fig. 1**

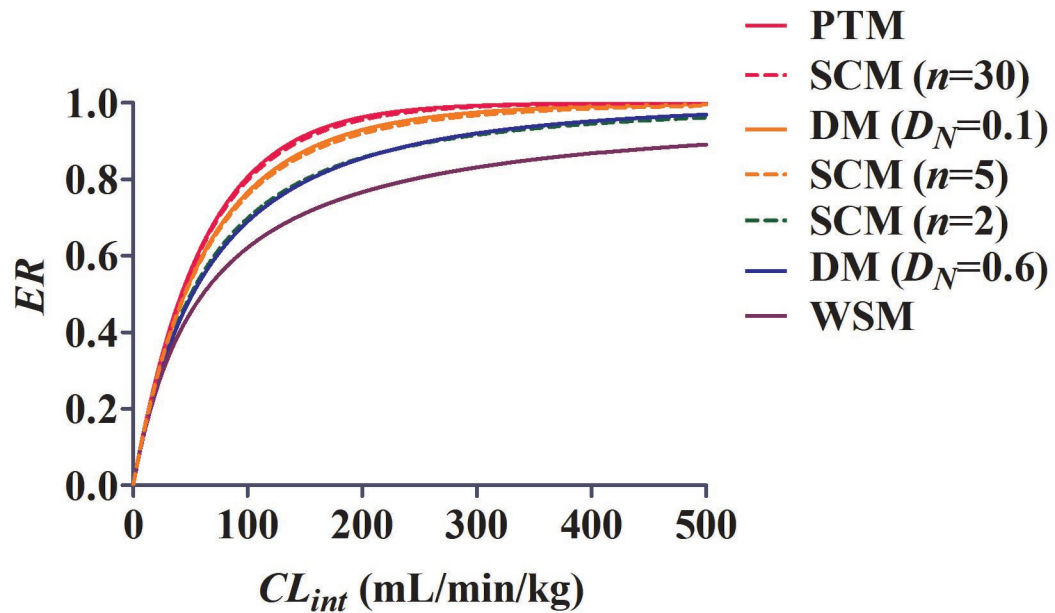


**Fig. 2**

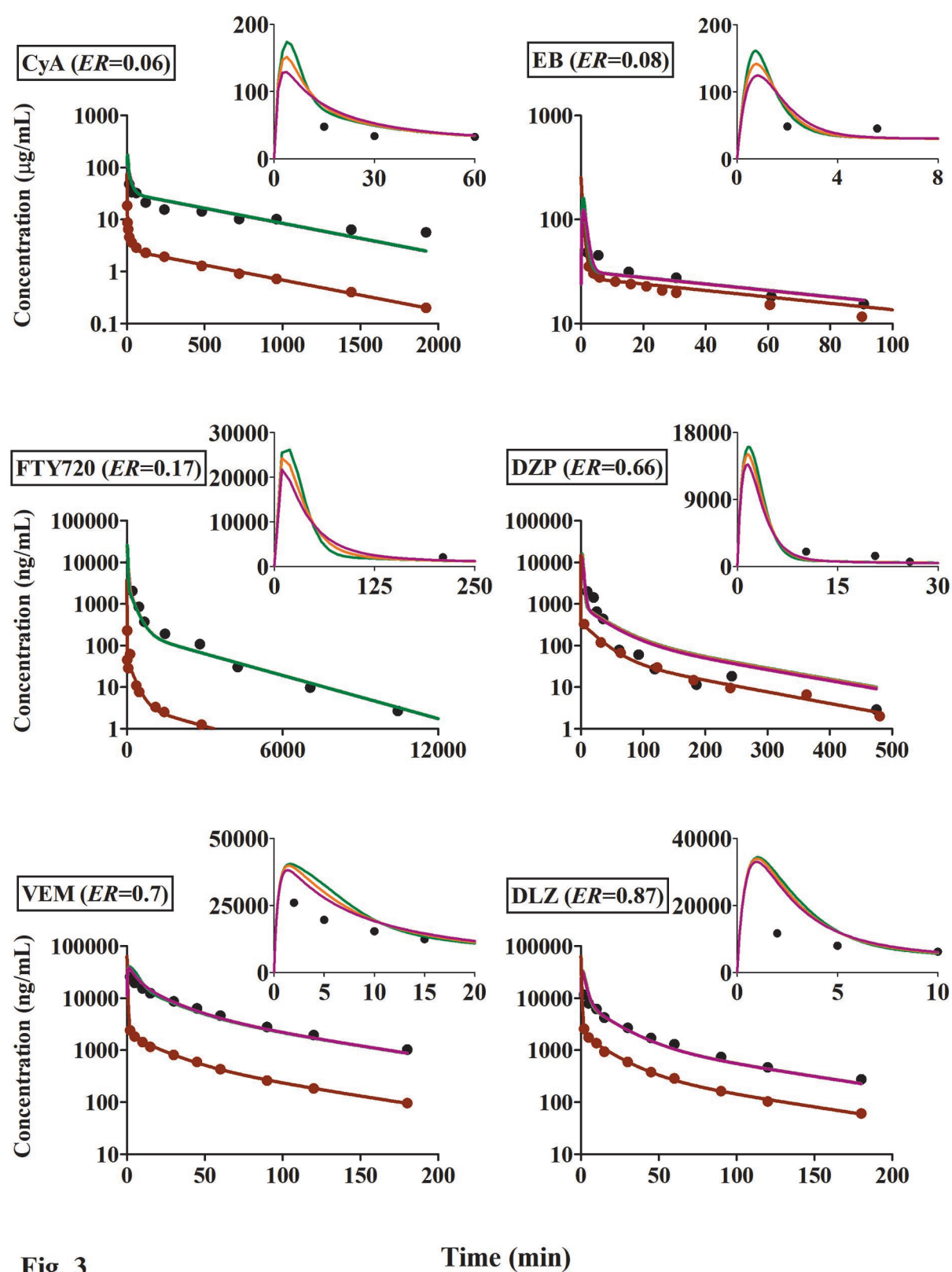
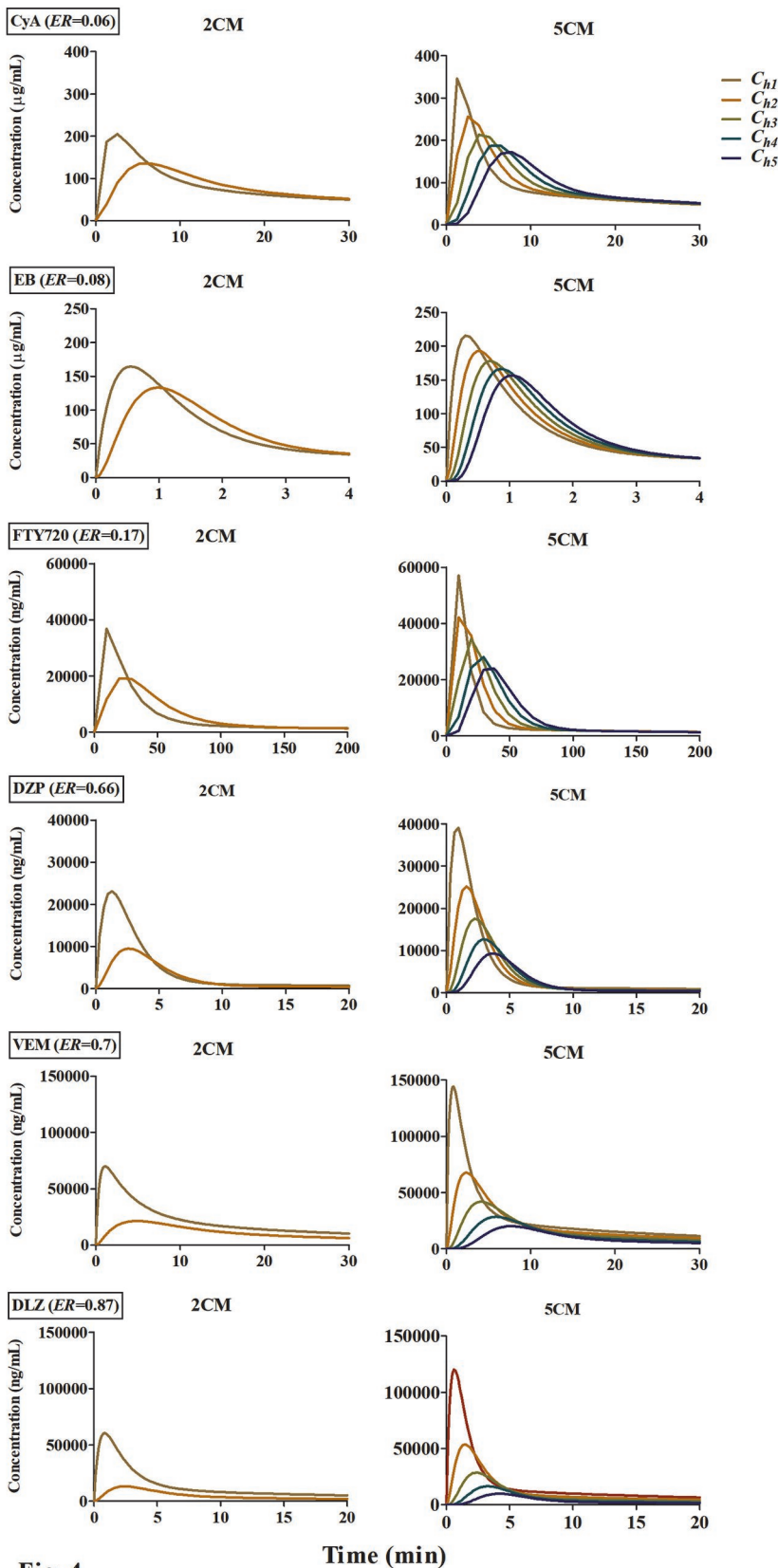
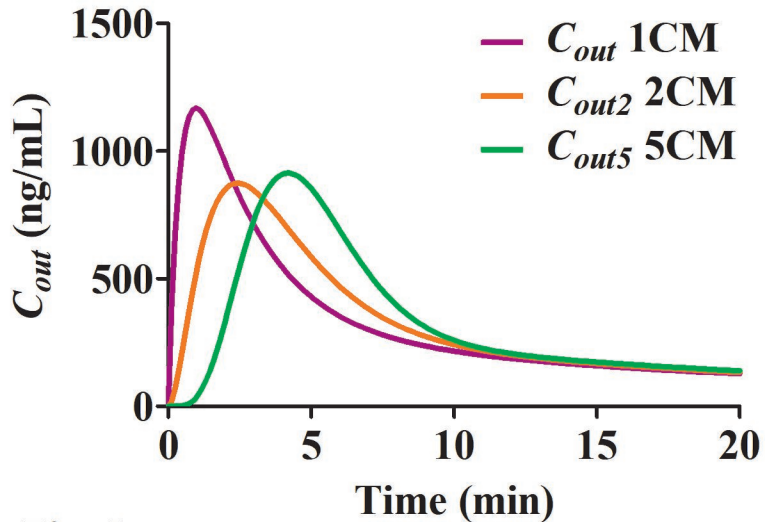


Fig. 3

Time (min)



**Fig. 4**



**Fig. 5**

**DLZ ( $ER=0.87$ )**

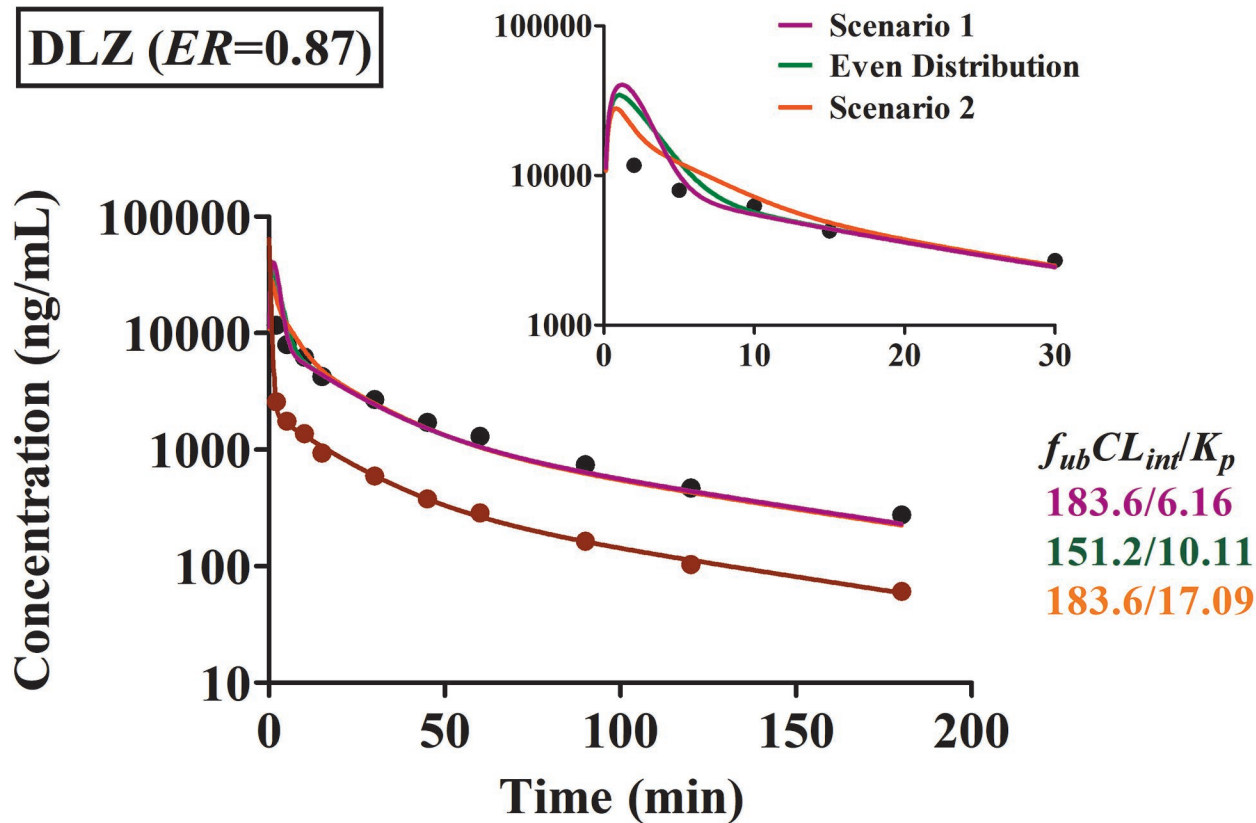


**Fig. 6**



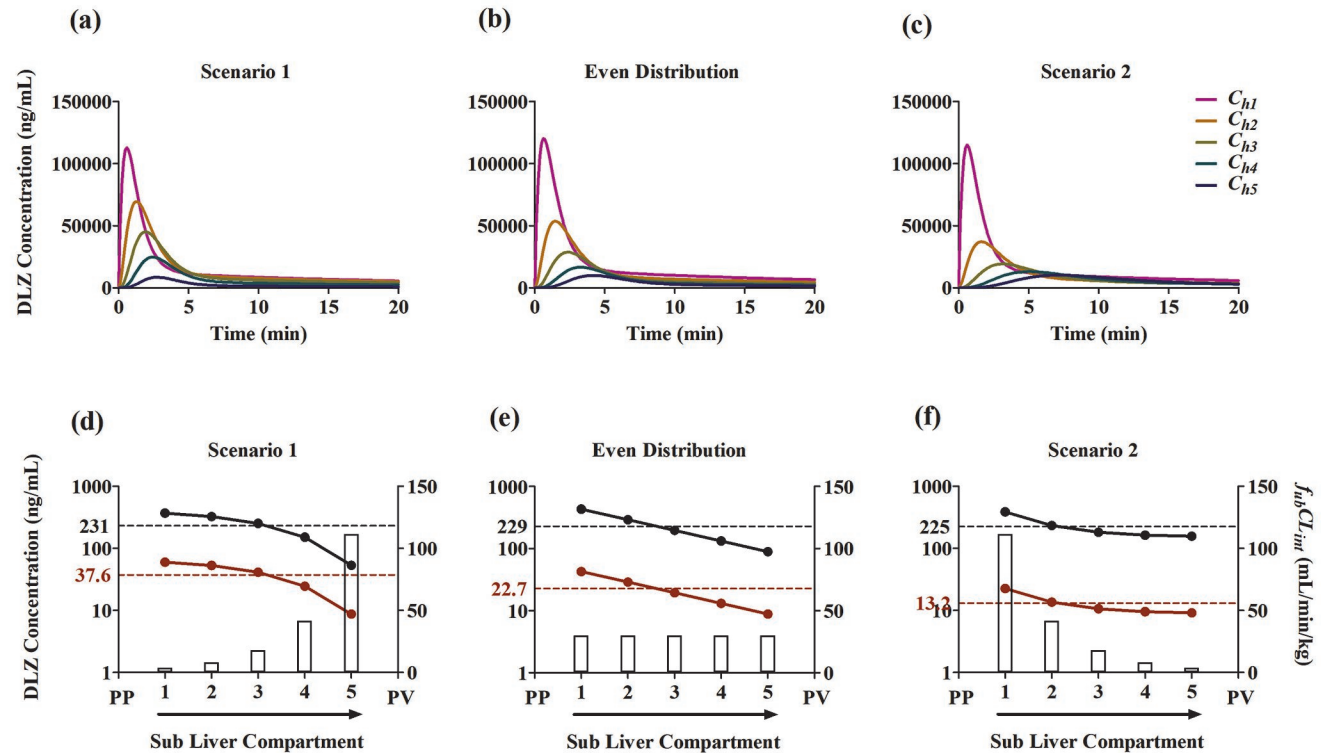
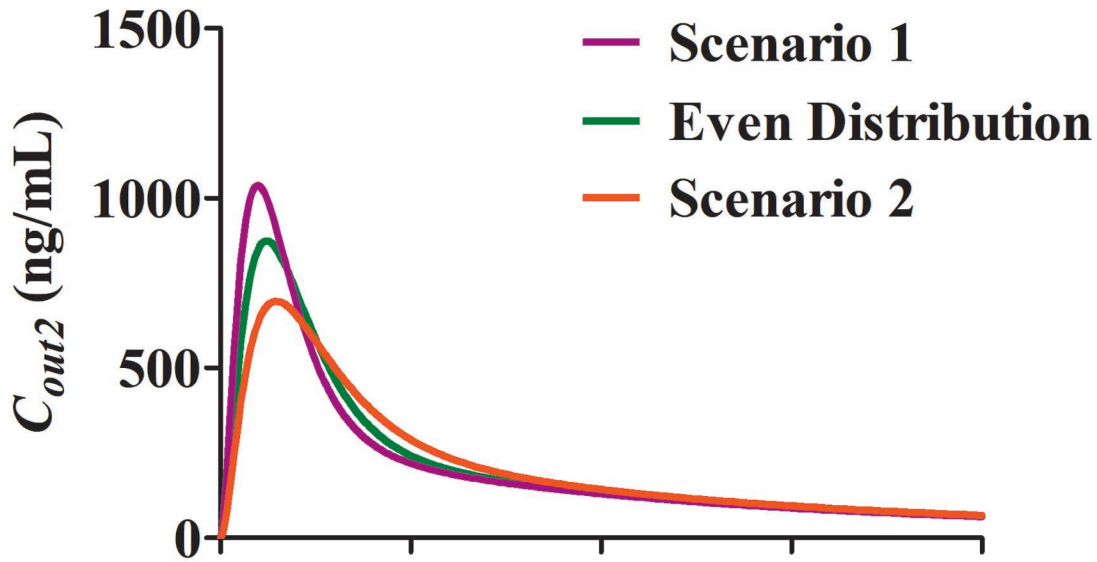


**Fig. 7**

**2CM**



**5CM**

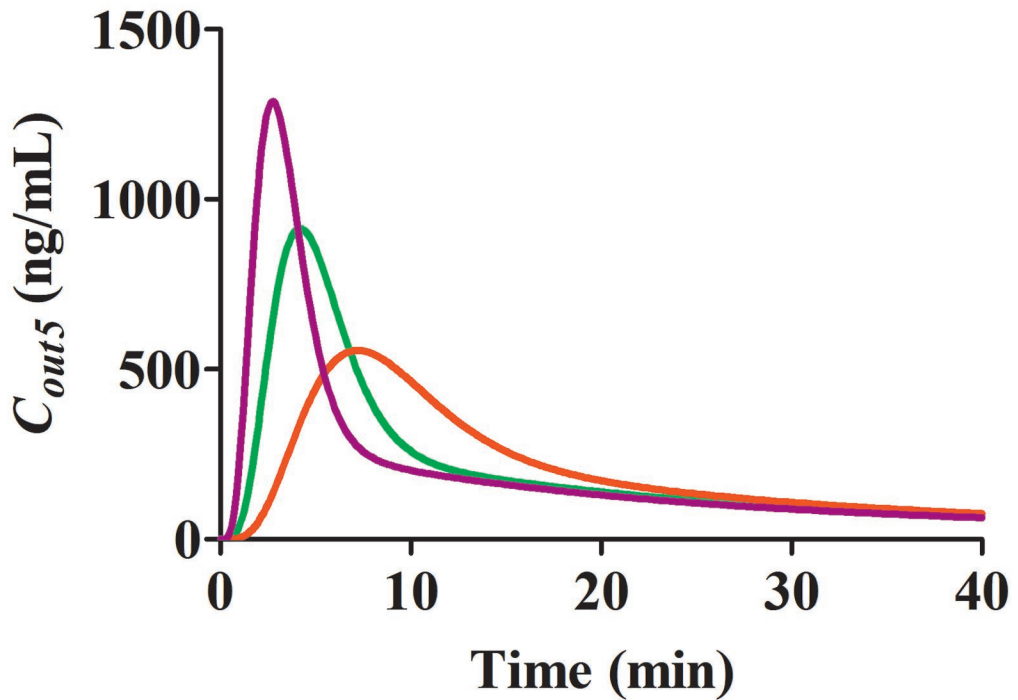


**Fig. 8**

DLZ ( $ER=0.87$ )

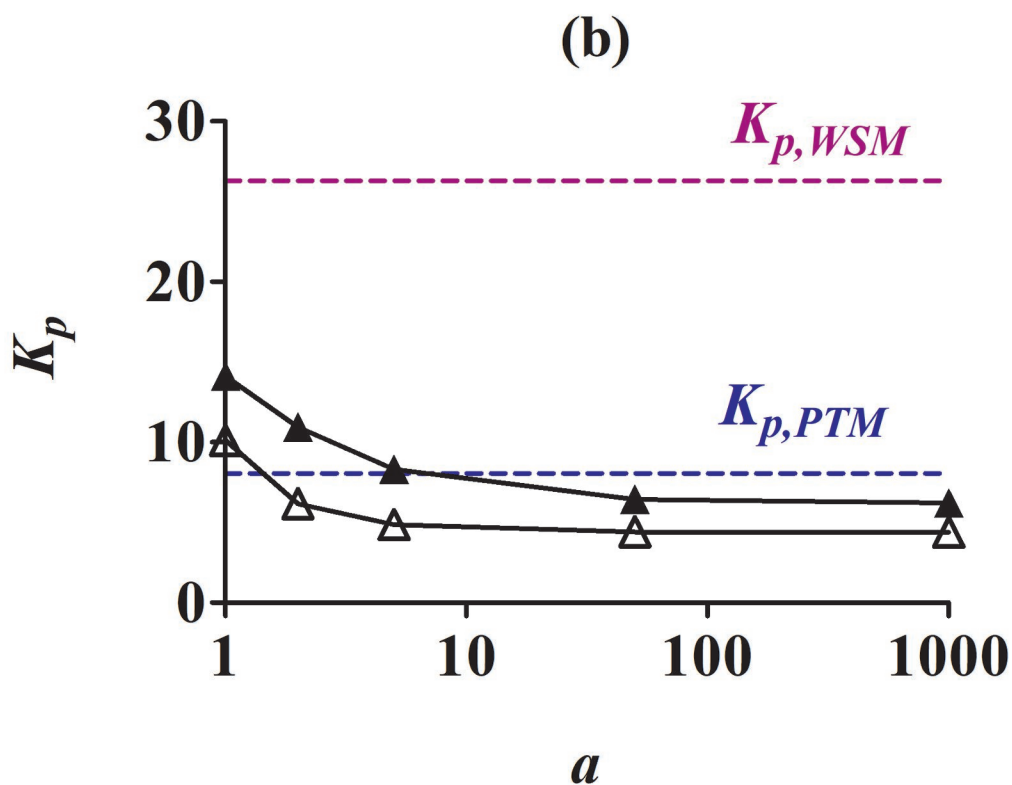
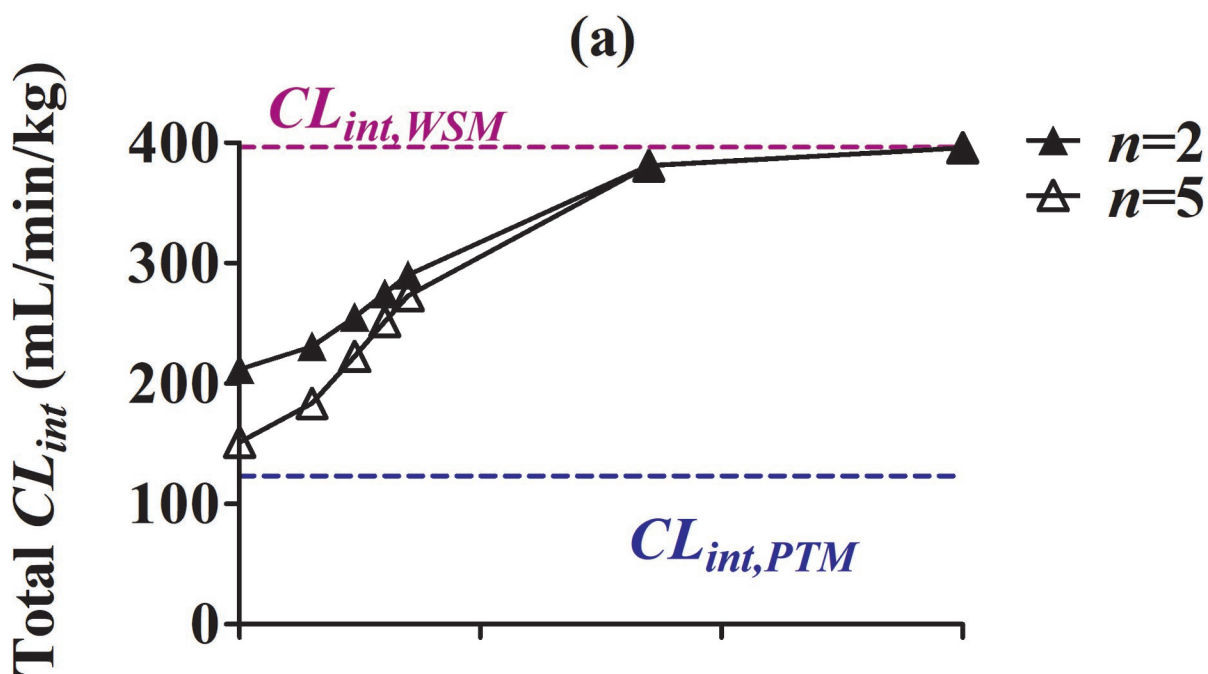


Fig. 9

## **Supplemental Materials**

**Manuscript number: DMD-AR-2022-001190**

**Title:**

**Exploring the Pharmacokinetic Mysteries of the Liver: Application of Series Compartment Models of Hepatic Elimination**

**Authors:**

Xiaonan Li and William J. Jusko

**Affiliation:**

Department of Pharmaceutical Sciences, State University of New York at Buffalo, 404 Pharmacy Building, Buffalo, New York 14214, USA

**Journal Title:**

Drug Metabolism and Disposition

## Supplemental Figures

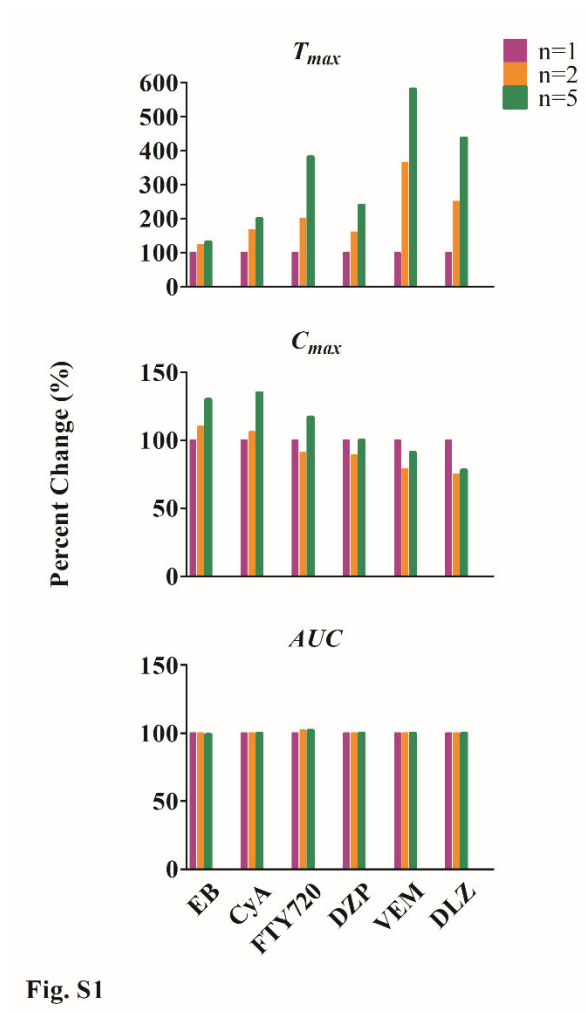
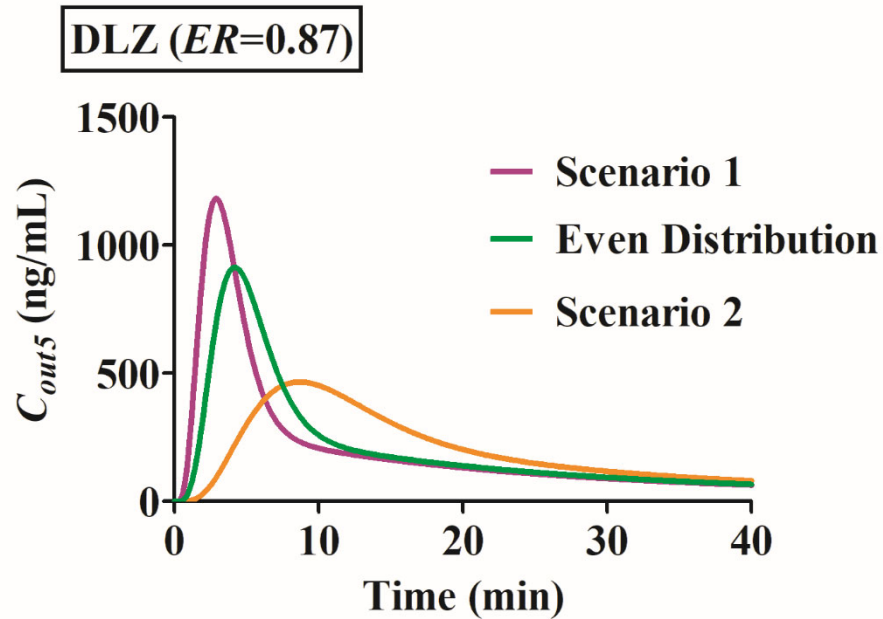


Fig. S1

Figure S1. Changes in  $T_{max}$ ,  $C_{max}$  and  $AUC$  of the predicted  $C_{outn}$ -time profiles for all compounds by the SCM as a function of numbers of compartments ( $n$ ) (percentage of those predicted by the SCM with  $n=1$ ).



**Figure S2. Outflow blood concentration-time profiles of DLZ from the last liver sub-compartment of the SCM as a function of hepatic enzyme zonation ( $a=1.6$  for Scenario 1 and  $1/1.6$  for Scenario 2).**

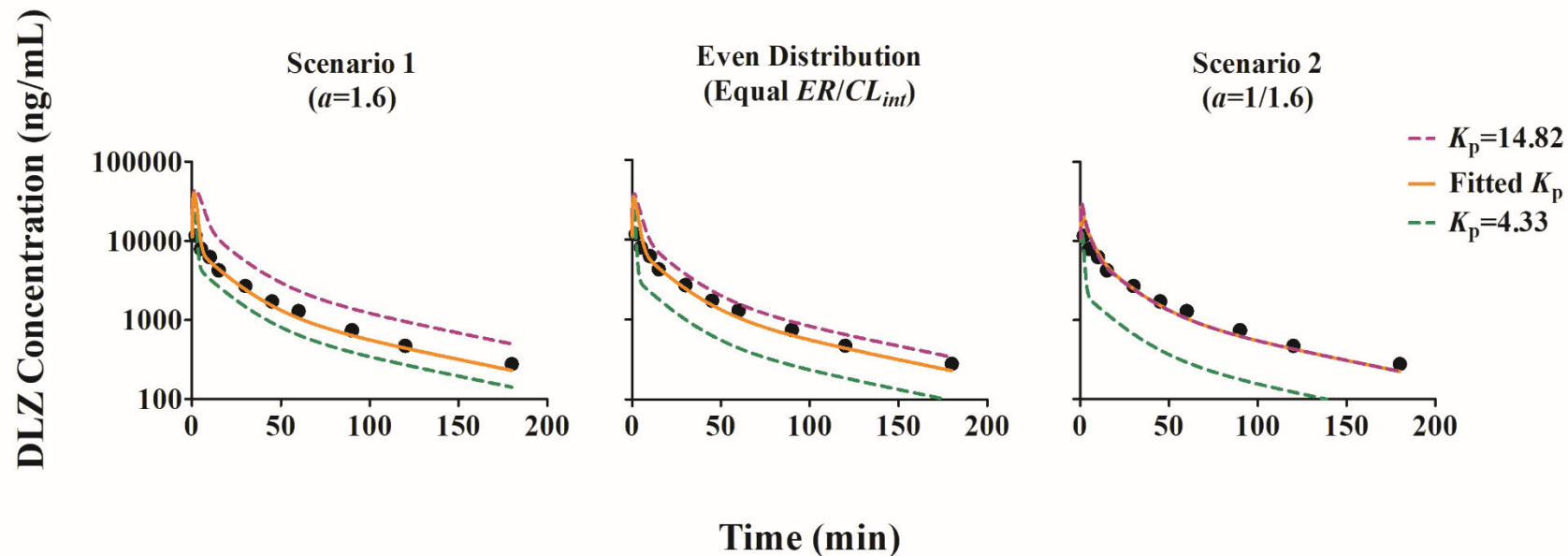


Fig. S3

Figure S3. Effects of changing  $K_p$  on predicting the liver concentration-time profiles of DLZ by the SCM with differing hepatic zonation ( $a=1.6$  and  $1/1.6$ ). Black circles are measured liver concentrations and color-coded dashed lines indicate model simulations with the corresponding model fitted  $K_p$  (6.97 for Scenario 1 and 14.9 for Scenario 2, purple) (Table S2), the lowest (M1  $K_{p,exp} = 4.33$ , green) and highest (M3  $K_{p,pred} = 14.82$ , purple) in silico  $K_p$  obtained from (Li and Jusko, 2022). In all cases, the metabolic intrinsic clearance in each of the sub compartments were fixed to the model-specific values listed in Table S2.

## Supplemental Tables

**Table S1.** Blood PK parameter estimates for the model compounds applying Eq. 16.

Compound	Intercepts (CV%) <sup>a</sup>			Slopes (1/min) (CV%)			Reference
	<i>A</i>	<i>B</i>	<i>C</i>	$\alpha$	$\beta$	$\gamma$	
CyA	60.34 (0.8)	5.06 (10.5)	2.6 (3.4)	0.894 (4.9)	0.047 (14.6)	0.0013 (2.4)	(Kawai et al., 1998)
EB	228.4 (0.4)	27.62 (3.5)		1.272 (10.4)	0.007 (6.5)		(Lin et al., 1978)
DZP	15140 (0.5)	205.2 (36.6)	44.62 (31.1)	0.935 (15)	0.0283 (34)	0.006 (13.8)	(Igari et al., 1983)
VEM	62040 (0.1)	1420 (5.4)	644.5 (12.8)	2.406 (4.1)	0.0466 (10.5)	0.0107 (7.6)	(Yamano et al., 2000)
DLZ	61990 (0.2)	1716 (6.3)	392.5 (16.2)	2.28 (5.9)	0.0566 (10.3)	0.0105 (10.4)	

<sup>a</sup> The units of the intercepts are the same as those of the blood concentrations for each of the model compounds shown in Figure 3; The sum of the intercepts was fixed as Dose/ $V_b$ .



Table S2. Parameters obtained from fitting the liver data of DLZ by the SCM with zonal and even distribution of hepatic enzymes ( $a$  was assigned to be 1.6 or 1/1.6)

Parameter (Unit)	Estimates (CV%)		
	Scenario 1	Scenario 2	Even Distribution
	(Lower PP $ER/CL_{int}$ )	(Lower PV $ER/CL_{int}$ )	(Equal $ER/CL_{int}$ )
$f_{ub}CL_{int1}$ (mL/min/kg) <sup>a</sup>	8.28	79.54	
$f_{ub}CL_{int2}$ (mL/min/kg) <sup>a</sup>	13.78	41.76	
$f_{ub}CL_{int3}$ (mL/min/kg) <sup>a</sup>	23.5	23.5	30.24 <sup>b</sup>
$f_{ub}CL_{int4}$ (mL/min/kg) <sup>a</sup>	41.76	13.78	
$f_{ub}CL_{int5}$ (mL/min/kg) <sup>a</sup>	79.54	8.28	
$f_{ub}CL_{int}$ (mL/min/kg) <sup>a</sup>	166.8		151.2 (8.2)
$K_p$	6.97 (7.08)	14.9 (6.85)	10.11 (7.3)
$T_{max}$ (min)	1.21	0.85	1.09
$C_{max}$ (ng/mL)	38793	29869	34339
$AUC_{inf}$ (ng*hr/mL)	362258	351530	358774
AIC	158.8	157.3	159

<sup>a</sup>  $f_{ub}CL_{inti}$  ( $i=1,2,...5$ ) was calculated from  $ER$  of DLZ using Eq. 3-4, 20-23 and fixed in the model fitting of liver data;  $f_{ub}CL_{int}$  is the sum of  $f_{ub}CL_{inti}$  of all liver compartments.

## Supplemental References

- Igari Y, Sugiyama Y, Sawada Y, Iga T, and Hanano M (1983) Prediction of diazepam disposition in the rat and man by a physiologically based pharmacokinetic model. *J Pharmacokinet Biopharm* **11**:577-593.
- Kawai R, Mathew D, Tanaka C, and Rowland M (1998) Physiologically based pharmacokinetics of cyclosporine A: Extension to tissue distribution kinetics in rats and scale-up to human. *J Pharmacol Exp Ther* **287**:457-468.
- Li X and Jusko WJ (2022) Assessing liver-to-plasma partition coefficients and in silico calculation methods: when does the hepatic model matter in PBPK? *Drug Metab Dispos*.
- Lin JH, Hayashi M, Awazu S, and Hanano M (1978) Correlation between in vitro and in vivo drug metabolism rate: oxidation of ethoxybenzamide in rat. *J Pharmacokinet Biopharm* **6**:327-337.
- Yamano K, Yamamoto K, Kotaki H, Takedomi S, Matsuo H, Sawada Y, and Iga T (2000) Quantitative prediction of metabolic inhibition of midazolam by erythromycin, diltiazem, and verapamil in rats: implication of concentrative uptake of inhibitors into liver. *J Pharmacol Exp Ther* **292**:1118-1126.

## Supplemental Methods

### ADAPT code for blood PK model (DLZ)

```

*****
C                      ADAPT                      *
C                      Version 5                  *
C*****
C                      *
C                      MODEL                      *
C                      *
C                      *
C      This file contains Fortran subroutines into which the user *
C      must enter the relevant model equations and constants.    *
C      Consult the User's Guide for details concerning the format for *
C      entered equations and definition of symbols.              *
C                      *
C      1. Symbol-   Parameter symbols and model constants        *
C      2. DiffEq-   System differential equations                 *
C      3. Output-   System output equations                       *
C      4. Varmod-   Error variance model equations                *
C      5. Covmod-   Covariate model equations (ITS,MLEM)          *
C      6. Popinit-  Population parameter initial values (ITS,MLEM) *
C      7. Prior -   Parameter mean and covariance values (ID,NPD,STS) *
C      8. Sparam-   Secondary parameters                          *
C      9. Amat -    System state matrix                           *
C                      *
C*****
C#####C

      Subroutine SYMBOL
      Implicit None

      Include 'globals.inc'
      Include 'model.inc'

```

```

CC
C-----C
C   Enter as Indicated                                     C
C---c-----C

```

```

NDEqs   = 0   ! Enter # of Diff. Eqs.
NSParam = 5   ! Enter # of System Parameters.
NVparam = 2   ! Enter # of Variance Parameters.
NSecPar = 9   ! Enter # of Secondary Parameters.
NSecOut = 0   ! Enter # of Secondary Outputs (not used).
Ieqsol  = 3   ! Model type: 1 - DIFFEQ, 2 - AMAT, 3 - OUTPUT only.
Descr   = '3CM iv blood/plasma data fit ER (Dose/AUC) '

```

```

CC
C-----C
C   Enter Symbol for Each System Parameter (eg. Psym(1)='Kel') C
C---c-----C

```

```

PSym(1) = 'C1'
PSym(2) = 'C2'
PSym(3) = 'alpha'
PSym(4) = 'beta'
PSym(5) = 'gamma'

```

```

CC
C-----C
C   Enter Symbol for Each Variance Parameter {eg: PVsym(1)='Sigma'} C
C---c-----C

```

```

PVsym(1)='Intercept'
PVsym(2)='Sigma'

```

```

CC

```

```

C-----C
C   Enter Symbol for Each Secondary Parameter {eg: PSsym(1)='CLt' }      C
C-----C
      PSsym(1)='AUCb'
      PSsym(2)='CLh'
      PSsym(3)='ER'
      PSsym(4)='CLint,WSM'
      PSsym(5)='CLint,PTM'
      PSsym(6)='AUCp'
      PSsym(7)='C3'
      PSsym(8)='CLint,5liver'
      PSsym(9)='CLint,2liver'

C-----C
C-----C
C
      Return
      End

C#####C

      Subroutine DIFFEQ(T,X,XP)
      Implicit None

      Include 'globals.inc'
      Include 'model.inc'

      Real*8 T,X(MaxNDE),XP(MaxNDE)

CC
C-----C
C   Enter Differential Equations Below {e.g.  XP(1) = -P(1)*X(1) }      C
C-----C

```

```

C-----C
C-----C
C
      Return
      End

C#####C

      Subroutine OUTPUT(Y,T,X)
      Implicit None

      Include 'globals.inc'
      Include 'model.inc'

      Real*8 Y(MaxNOE),T,X(MaxNDE)
      Real*8 C1,C2,alpha,beta,Fig,ka,C3,gamma
CC
C-----C
C   Enter Output Equations Below   {e.g.  Y(1) = X(1)/P(2) }   C
C-----C

      C1  = P(1)
      C2  = P(2)
      alpha= P(3)
      beta = P(4)
      C3=64102.56-C1-C2
      gamma=P(5)
      Y(1)=C1*exp(-alpha*T)+C2*exp(-beta*T)+C3*exp(-gamma*T) ! blood

C-----C
C-----C
C
      Return

```

End

C#####C

Subroutine VARMOD(V,T,X,Y)

Implicit None

Include 'globals.inc'

Include 'model.inc'

Real\*8 V(MaxNOE),T,X(MaxNDE),Y(MaxNOE)

Real\*8 Sigma,Intercept

CC

C-----C

C Enter Variance Model Equations Below C

C {e.g. V(1) = (PV(1) + PV(2)\*Y(1))\*\*2 } C

C---C-----C

Intercept=PV(1)

Sigma=PV(2)

V(1)= (PV(1)+PV(2)\*Y(1))\*\*2

C-----C

C-----C

C

Return

End

C#####C

Subroutine COVMOD(Pmean, ICmean, PC)

C Defines any covariate model equations (MLEM, ITS)

Implicit None

```

      Include 'globals.inc'
      Include 'model.inc'

      Real*8 PC(MaxNCP)
      Real*8 Pmean(MaxNSP+MaxNDE), ICmean(MaxNDE)

CC
C-----C
C      Enter # of Covariate Parameters                                C
C-----C-----C

      NCparam = 0      ! Enter # of Covariate Parameters.

CC
C-----C
C      Enter Symbol for Covariate Params {eg: PCsym(1)='CLRenal'}    C
C-----C-----C

CC
C-----C
C      For the Model Params. that Depend on Covariates Enter the Equation C
C      {e.g. Pmean(1) = PC(1)*R(2) }                                C
C-----C-----C

C-----C
C-----C
C
      Return
      End

C#####C

```



```

      Subroutine POPINIT(PmeanI,ICmeanI,PcovI,ICcovI, PCI)
C   Initial parameter values for population program parameters (ITS, MLEM)

      Implicit None

      Include 'globals.inc'
      Include 'model.inc'

      Integer I,J
      Real*8 PmeanI(MaxNSP+MaxNDE), ICmeanI(MaxNDE)
      Real*8 PcovI(MaxNSP+MaxNDE,MaxNSP+MaxNDE), ICcovI(MaxNDE,MaxNDE)
      Real*8 PCI(MaxNCP)

CC
C-----C
C   Enter Initial Values for Population Means                C
C       {   e.g. PmeanI(1) = 10.0       }                    C
C-----C-----C

CC
C-----C
C   Enter Initial Values for Pop. Covariance Matrix (Lower Triang.) C
C       {   e.g. PcovI(2,1) = 0.25       }                    C
C-----C-----C

CC
C-----C
C   Enter Values for Covariate Model Parameters              C
C       {   e.g. PCI(1) = 2.0       }                          C
C-----C-----C

```

```

C-----C
C-----C
C
      Return
      End

C#####C

      Subroutine PRIOR(Pmean,Pcov,ICmean,ICcov)
C  Parameter mean and covariance values for MAP estimation (ID,NPD,STS)
      Implicit None

      Include 'globals.inc'
      Include 'model.inc'

      Integer I,J
      Real*8 Pmean(MaxNSP+MaxNDE), ICmean(MaxNDE)
      Real*8 Pcov(MaxNSP+MaxNDE,MaxNSP+MaxNDE), ICcov(MaxNDE,MaxNDE)

CC
C-----C
C  Enter Nonzero Elements of Prior Mean Vector      C
C      { e.g. Pmean(1) = 10.0      }      C
C-----C

CC
C-----C
C  Enter Nonzero Elements of Covariance Matrix (Lower Triang.)      C
C      { e.g. Pcov(2,1) = 0.25      }      C
C-----C

C-----C

```

```

C-----C
C
      Return
      End

C#####C

      Subroutine SPARAM(PS,P,IC)
      Implicit None

      Include 'globals.inc'

      Real*8 PS(MaxNSECP), P(MaxNSP+MaxNDE), IC(MaxNDE)
      Real*8 C1,C2,alpha,beta,CLh,Dose,ER,CLint,Qliver,Rb,QliverBrown
      Real*8 C3,gamma

CC
C-----C
C   Enter Equations Defining Secondary Paramters           C
C   { e.g.   PS(1) = P(1)*P(2)   }                           C
C-----C
      C1 = P(1)
      C2 = P(2)
      alpha = P(3)
      beta = P(4)
      C3=64102.56-C1-C2
      gamma=P(5)

      QliverBrown=60.82
      Qliver=60.82 !no reported value

      Dose=5000000 !ng/kg
      Rb=0.93

```

```

      PS(1) = (C1/alpha+C2/beta+C3/gamma) !Blood AUC
      PS(2) = Dose/(C1/alpha+C2/beta+C3/gamma) !CLh
      PS(3) = (Dose/(C1/alpha+C2/beta+C3/gamma))/(Qliver) !ER
      PS(4) = QliverBrown*(PS(3)/(1-PS(3))) !CLint,WSM

      PS(5) = -QliverBrown*LOG(1-PS(3)) !CLint,PTM
      PS(6) = PS(1)/Rb !plamsa AUC
      PS(7) = C3
      PS(8) = 5*(QliverBrown*(1-(1-PS(3))**0.2)/(1-PS(3))**0.2) !CLint for 5 liver
comp
      PS(9) = 2*(QliverBrown*(1-(1-PS(3))**0.5)/(1-PS(3))**0.5) !CLint for 2 liver
comp

C-----C
C-----C
C
      Return
      End

C#####C

      Subroutine AMAT(A)
      Implicit None

      Include 'globals.inc'
      Include 'model.inc'

      Integer I,J
      Real*8 A(MaxNDE,MaxNDE)

      DO I=1,Ndeqs
        Do J=1,Ndeqs
          A(I,J)=0.0D0

```

End Do  
End Do

CC  
C-----C  
C Enter non zero elements of state matrix {e.g.  $A(1,1) = -P(1)$  } C  
C---C-----C

C-----C  
C-----C  
C

Return  
End

C#####C

**ADAPT code for the SCM with  $n=1$  (DLZ)**

```

*****
C                                ADAPT                                *
C                                Version 5                            *
C*****
C                                *
C                                MODEL                                *
C                                *
C                                *
C    This file contains Fortran subroutines into which the user      *
C    must enter the relevant model equations and constants.          *
C    Consult the User's Guide for details concerning the format for  *
C    entered equations and definition of symbols.                     *
C                                *
C    1. Symbol-   Parameter symbols and model constants              *
C    2. DiffEq-   System differential equations                      *
C    3. Output-   System output equations                            *
C    4. Varmod-   Error variance model equations                    *
C    5. Covmod-   Covariate model equations (ITS,MLEM)              *
C    6. Popinit-  Population parameter initial values (ITS,MLEM)    *
C    7. Prior -   Parameter mean and covariance values (ID,NPD,STS) *
C    8. Sparam-   Secondary parameters                              *
C    9. Amat  -   System state matrix                                *
C                                *
C*****
C#####C

Subroutine SYMBOL
Implicit None

Include 'globals.inc'
Include 'model.inc'

CC

```

```

C-----C
C   Enter as Indicated                               C
C---C-----C

```

```

NDEqs   = 1   ! Enter # of Diff. Eqs.
NSParam = 1   ! Enter # of System Parameters.
NVparam = 2   ! Enter # of Variance Parameters.
NSecPar = 0   ! Enter # of Secondary Parameters.
NSecOut = 0   ! Enter # of Secondary Outputs (not used).
Ieqsol  = 1   ! Model type: 1 - DIFFEQ, 2 - AMAT, 3 - OUTPUT only.
Descr   = ' DLZ 1CM S1-1 '

```

```

CC
C-----C
C   Enter Symbol for Each System Parameter (eg. Psym(1)='Kel')   C
C---C-----C

```

```

      PSym(1) = 'Kp'

```

```

CC
C-----C
C   Enter Symbol for Each Variance Parameter {eg: PVsym(1)='Sigma'}   C
C---C-----C

```

```

      PVsym(1)='Intercept'
      PVsym(2)='Sigma'

```

```

CC
C-----C
C   Enter Symbol for Each Secondary Parameter {eg: PSsym(1)='CLt'}   C
C---C-----C

```

```

C-----C
C-----C
C
      Return
      End

C#####C

      Subroutine DIFFEQ(T,X,XP)
      Implicit None

      Include 'globals.inc'
      Include 'model.inc'

      Real*8 T,X(MaxNDE),XP(MaxNDE)
      Real*8 C1,C2,ka,alpha,beta,Carl,Cout1,Cout2,Cout3,Cout4,Cout5
      Real*8 Qliver,Vliver,Kp,Rb,fub,CLint,ER,DN,a,C3,gamma,F,Fi

CC
C-----C
C   Enter Differential Equations Below   {e.g.  XP(1) = -P(1)*X(1) }   C
C---C-----C

      Kp=P(1)

      Qliver=60.82 !mL/min/kg
      Vliver=36.6 !mL/kg
      Rb=0.93
      ER=0.867
      CLint=397 !1CM SCM

C Fixed parameters:

```



```

C1  = 61990
C2=1716
alpha =2.28
beta=0.05659
gamma=0.01052
C3=392.5

```

```

Cart=C1*exp(-alpha*T)+C2*exp(-beta*T)+C3*exp(-gamma*T) ! blood

```

```

XP(1)=(Qliver*(Cart-Rb*X(1)/(Kp))
x      -(CLint)*Rb*X(1)/(Kp)) / (Vliver)

```

```

C-----C
C-----C
C

```

```

Return
End

```

```

C#####C

```

```

Subroutine OUTPUT(Y,T,X)
Implicit None

```

```

Include 'globals.inc'
Include 'model.inc'

```

```

Real*8 Y(MaxNOE),T,X(MaxNDE)

```

```

CC
C-----C
C  Enter Output Equations Below {e.g. Y(1) = X(1)/P(2) } C
C---C-----C

```

```

          Y(1)=X(1)          ! liver

C-----C
C-----C
C
      Return
      End

C#####C

      Subroutine VARMOD(V,T,X,Y)
      Implicit None

      Include 'globals.inc'
      Include 'model.inc'

      Real*8 V(MaxNOE),T,X(MaxNDE),Y(MaxNOE)
      Real*8 Sigma,Intercept

CC
C-----C
C   Enter Variance Model Equations Below           C
C       {e.g. V(1) = (PV(1) + PV(2)*Y(1))**2 }      C
C-----C
      Intercept=PV(1)
      Sigma=PV(2)

      V(1)= (PV(1)+PV(2)*Y(1))**2

C-----C
C-----C
C
      Return

```

End

C#####C

Subroutine COVMOD(Pmean, ICmean, PC)

C Defines any covariate model equations (MLEM, ITS)

Implicit None

Include 'globals.inc'

Include 'model.inc'

Real\*8 PC(MaxNCP)

Real\*8 Pmean(MaxNSP+MaxNDE), ICmean(MaxNDE)

CC

C-----C

C Enter # of Covariate Parameters C

C---C-----C

NCparam = 0 ! Enter # of Covariate Parameters.

CC

C-----C

C Enter Symbol for Covariate Params {eg: PCsym(1)='CLRenal'} C

C---C-----C

CC

C-----C

C For the Model Params. that Depend on Covariates Enter the Equation C

C {e.g. Pmean(1) = PC(1)\*R(2) } C

C---C-----C

```

C-----C
C-----C
C
      Return
      End

C#####C

      Subroutine POPINIT(PmeanI,ICmeanI,PcovI,ICcovI, PCI)
C  Initial parameter values for population program parameters (ITS, MLEM)

      Implicit None

      Include 'globals.inc'
      Include 'model.inc'

      Integer I,J
      Real*8 PmeanI(MaxNSP+MaxNDE), ICmeanI(MaxNDE)
      Real*8 PcovI(MaxNSP+MaxNDE,MaxNSP+MaxNDE), ICcovI(MaxNDE,MaxNDE)
      Real*8 PCI(MaxNCP)

CC
C-----C
C  Enter Initial Values for Population Means      C
C      { e.g. PmeanI(1) = 10.0      }      C
C-----C-----C

CC
C-----C
C  Enter Initial Values for Pop. Covariance Matrix (Lower Triang.)      C
C      { e.g. PcovI(2,1) = 0.25      }      C
C-----C-----C

```

```

CC
C-----C
C   Enter Values for Covariate Model Parameters      C
C           {   e.g. PCI(1) = 2.0           }      C
C-----C-----C

C-----C
C-----C
C
      Return
      End

C#####C

      Subroutine PRIOR(Pmean,Pcov,ICmean,ICcov)
C   Parameter mean and covariance values for MAP estimation (ID,NPD,STS)
      Implicit None

      Include 'globals.inc'
      Include 'model.inc'

      Integer I,J
      Real*8 Pmean(MaxNSP+MaxNDE), ICmean(MaxNDE)
      Real*8 Pcov(MaxNSP+MaxNDE,MaxNSP+MaxNDE), ICcov(MaxNDE,MaxNDE)

CC
C-----C
C   Enter Nonzero Elements of Prior Mean Vector      C
C           {   e.g. Pmean(1) = 10.0           }      C
C-----C-----C

```

```

CC
C-----C
C   Enter Nonzero Elements of Covariance Matrix (Lower Triang.)      C
C       {   e.g. Pcov(2,1) = 0.25      }                             C
C-----C-----C

```

```

C-----C
C-----C
C
      Return
      End

```

```

C#####C

```

```

      Subroutine SPARAM(PS,P,IC)
      Implicit None

```

```

      Include 'globals.inc'

```

```

      Real*8 PS(MaxNSECP), P(MaxNSP+MaxNDE), IC(MaxNDE)
      Real*8 ER,F,Fi,CLinti,CLint

```

```

CC
C-----C
C   Enter Equations Defining Secondary Paramters                    C
C       {   e.g.   PS(1) = P(1)*P(2)      }                         C
C-----C-----C

```

```

C-----C
C-----C

```

C

```

      Return
      End

```

C#####C

```

      Subroutine AMAT(A)
      Implicit None

```

```

      Include 'globals.inc'
      Include 'model.inc'

```

```

      Integer I,J
      Real*8 A(MaxNDE,MaxNDE)

```

```

      DO I=1,Ndeqs
        Do J=1,Ndeqs
          A(I,J)=0.0D0
        End Do
      End Do

```

CC

```

C-----C
C   Enter non zero elements of state matrix  {e.g.  A(1,1) = -P(1) }   C
C---c-----C

```

```

C-----C
C-----C
C

```

```

      Return
      End

```

C#####C

**ADAPT code for the SCM with  $n=2$  (DLZ)**

```

*****
C                                ADAPT                                *
C                                Version 5                            *
C*****
C                                *
C                                MODEL                                *
C                                *
C                                *
C    This file contains Fortran subroutines into which the user      *
C    must enter the relevant model equations and constants.          *
C    Consult the User's Guide for details concerning the format for  *
C    entered equations and definition of symbols.                     *
C                                *
C    1. Symbol-   Parameter symbols and model constants              *
C    2. DiffEq-   System differential equations                       *
C    3. Output-   System output equations                             *
C    4. Varmod-   Error variance model equations                     *
C    5. Covmod-   Covariate model equations (ITS,MLEM)               *
C    6. Popinit-  Population parameter initial values (ITS,MLEM)     *
C    7. Prior -   Parameter mean and covariance values (ID,NPD,STS)  *
C    8. Sparam-   Secondary parameters                               *
C    9. Amat  -   System state matrix                                *
C                                *
C*****
C#####C

    Subroutine SYMBOL
    Implicit None

    Include 'globals.inc'
    Include 'model.inc'

CC

```



```

C-----C
C   Enter as Indicated                               C
C---C-----C

```

```

NDEqs   = 2    ! Enter # of Diff. Eqs.
NSParam = 1    ! Enter # of System Parameters.
NVparam = 2    ! Enter # of Variance Parameters.
NSecPar = 0    ! Enter # of Secondary Parameters.
NSecOut = 0    ! Enter # of Secondary Outputs (not used).
Ieqsol  = 1    ! Model type: 1 - DIFFEQ, 2 - AMAT, 3 - OUTPUT only.
Descr   = ' DLZ 2CM S1-1 new'

```

```

CC
C-----C
C   Enter Symbol for Each System Parameter (eg. Psym(1)='Kel')   C
C---C-----C

```

```

      PSym(1) = 'Kp'

```

```

CC
C-----C
C   Enter Symbol for Each Variance Parameter {eg: PVsym(1)='Sigma'}   C
C---C-----C

```

```

      PVsym(1)='Intercept'
      PVsym(2)='Sigma'

```

```

CC
C-----C
C   Enter Symbol for Each Secondary Parameter {eg: PSsym(1)='CLt'}   C
C---C-----C

```

```

C-----C

```

```

C-----C
C
      Return
      End

C#####C

      Subroutine DIFFEQ(T,X,XP)
      Implicit None

      Include 'globals.inc'
      Include 'model.inc'

      Real*8 T,X(MaxNDE),XP(MaxNDE)
      Real*8 C1,C2,ka,alpha,beta,Card,Cout1,Cout2,Cout3,Cout4,Cout5
      Real*8 Qliver,Vliver,Kp,Rb,fub,CLint,ER,DN,a,C3,gamma,F,Fi

CC
C-----C
C   Enter Differential Equations Below   {e.g.  XP(1) = -P(1)*X(1) }   C
C-----C-----C

      Kp=P(1)
      Qliver=60.82 !mL/min/kg
      Vliver=36.6 !mL/kg
      Rb=0.93
      ER=0.867
      CLint=211.9 !2CM SCM

C Fixed parameters:
      C1 = 61990
      C2=1716
      alpha =2.28

```

```

beta=0.05659
gamma=0.01052
C3=392.5

```

```

Cart=C1*exp(-alpha*T)+C2*exp(-beta*T)+C3*exp(-gamma*T)  ! blood

```

```

      XP(1)=(Qliver*(Cart-Rb*X(1)/(Kp))
x          -(CLint/2)*Rb*X(1)/(Kp)) / (Vliver/2)
      XP(2)=(Qliver*(Rb*X(1)/(Kp)-Rb*X(2)/(Kp))
x          -(CLint/2)*Rb*X(2)/(Kp)) / (Vliver/2)

```

```

C-----C
C-----C
C

```

```

      Return
      End

```

```

C#####C

```

```

      Subroutine OUTPUT(Y,T,X)
      Implicit None

```

```

      Include 'globals.inc'
      Include 'model.inc'

```

```

      Real*8 Y(MaxNOE),T,X(MaxNDE)

```

```

CC
C-----C
C  Enter Output Equations Below    {e.g.  Y(1) = X(1)/P(2) }      C
C-----C

```

```

      Y(1)=X(1)
      Y(2)=X(2)
      Y(3)=(X(1)+X(2))/2

```

```

C-----C
C-----C
C

```

```

      Return
      End

```

```

C#####C

```

```

      Subroutine VARMOD(V,T,X,Y)
      Implicit None

```

```

      Include 'globals.inc'
      Include 'model.inc'

```

```

      Real*8 V(MaxNOE),T,X(MaxNDE),Y(MaxNOE)
      Real*8 Sigma,Intercept

```

```

CC
C-----C
C   Enter Variance Model Equations Below           C
C       {e.g. V(1) = (PV(1) + PV(2)*Y(1))**2 }      C
C-----C

```

```

      Intercept=PV(1)
      Sigma=PV(2)

```

```

      V(1:3) = (PV(1)+PV(2)*Y(1:3))**2

```

```

C-----C
C-----C
C

```

```

Return
End

```

```

C#####C

```

```

      Subroutine COVMOD(Pmean, ICmean, PC)
C  Defines any covariate model equations (MLEM, ITS)
      Implicit None

```

```

      Include 'globals.inc'
      Include 'model.inc'

```

```

      Real*8 PC(MaxNCP)
      Real*8 Pmean(MaxNSP+MaxNDE), ICmean(MaxNDE)

```

```

CC
C-----C
C      Enter # of Covariate Parameters                      C
C----c-----C

```

```

      NCparam = 0      ! Enter # of Covariate Parameters.

```

```

CC
C-----C
C      Enter Symbol for Covariate Params {eg: PCsym(1)='CLRenal'}      C
C----c-----C

```

```

CC
C-----C
C      For the Model Params. that Depend on Covariates Enter the Equation C
C      {e.g. Pmean(1) = PC(1)*R(2) }                      C
C----c-----C

```

```

C-----C
C-----C
C
      Return
      End

C#####C

      Subroutine POPINIT(PmeanI,ICmeanI,PcovI,ICcovI, PCI)
C  Initial parameter values for population program parameters (ITS, MLEM)

      Implicit None

      Include 'globals.inc'
      Include 'model.inc'

      Integer I,J
      Real*8 PmeanI(MaxNSP+MaxNDE), ICmeanI(MaxNDE)
      Real*8 PcovI(MaxNSP+MaxNDE,MaxNSP+MaxNDE), ICcovI(MaxNDE,MaxNDE)
      Real*8 PCI(MaxNCP)

CC
C-----C
C  Enter Initial Values for Population Means      C
C      { e.g. PmeanI(1) = 10.0      }      C
C---c-----C

CC
C-----C
C  Enter Initial Values for Pop. Covariance Matrix (Lower Triang.)  C
C      { e.g. PcovI(2,1) = 0.25      }      C
C---c-----C

```

```

CC
C-----C
C   Enter Values for Covariate Model Parameters      C
C       {   e.g. PCI(1) = 2.0       }                C
C-----C-----C

C-----C
C-----C
C
      Return
      End

C#####C

      Subroutine PRIOR(Pmean,Pcov,ICmean,ICcov)
C   Parameter mean and covariance values for MAP estimation (ID,NPD,STS)
      Implicit None

      Include 'globals.inc'
      Include 'model.inc'

      Integer I,J
      Real*8 Pmean(MaxNSP+MaxNDE), ICmean(MaxNDE)
      Real*8 Pcov(MaxNSP+MaxNDE,MaxNSP+MaxNDE), ICcov(MaxNDE,MaxNDE)

CC
C-----C
C   Enter Nonzero Elements of Prior Mean Vector      C
C       {   e.g. Pmean(1) = 10.0       }                C
C-----C-----C

```

```

CC
C-----C
C   Enter Nonzero Elements of Covariance Matrix (Lower Triang.)      C
C       {   e.g. Pcov(2,1) = 0.25   }                                C
C-----C

C-----C
C-----C
C
      Return
      End

C#####C

      Subroutine SPARAM(PS,P,IC)
      Implicit None

      Include 'globals.inc'

      Real*8 PS(MaxNSECP), P(MaxNSP+MaxNDE), IC(MaxNDE)
      Real*8 ER,F,Fi,CLinti,CLint

CC
C-----C
C   Enter Equations Defining Secondary Paramters                      C
C       {   e.g.   PS(1) = P(1)*P(2)   }                              C
C-----C

C-----C
C-----C
C

```



```

      Return
      End

```

```

C#####C

```

```

      Subroutine AMAT(A)
      Implicit None

```

```

      Include 'globals.inc'
      Include 'model.inc'

```

```

      Integer I,J
      Real*8 A(MaxNDE,MaxNDE)

```

```

      DO I=1,Ndeqs
        Do J=1,Ndeqs
          A(I,J)=0.0D0
        End Do
      End Do

```

```

CC

```

```

C-----C
C   Enter non zero elements of state matrix   {e.g.  A(1,1) = -P(1) }   C
C---C-----C

```

```

C-----C
C-----C
C

```

```

      Return
      End

```

```

C#####C

```

**ADAPT code for the SCM with  $n=5$  (DLZ)**

```

*****
C                                ADAPT                                *
C                                Version 5                            *
C*****
C                                *
C                                MODEL                                *
C                                *
C                                *
C    This file contains Fortran subroutines into which the user      *
C    must enter the relevant model equations and constants.          *
C    Consult the User's Guide for details concerning the format for  *
C    entered equations and definition of symbols.                     *
C                                *
C    1. Symbol-   Parameter symbols and model constants              *
C    2. DiffEq-   System differential equations                      *
C    3. Output-   System output equations                            *
C    4. Varmod-   Error variance model equations                    *
C    5. Covmod-   Covariate model equations (ITS,MLEM)              *
C    6. Popinit-  Population parameter initial values (ITS,MLEM)    *
C    7. Prior -   Parameter mean and covariance values (ID,NPD,STS) *
C    8. Sparam-   Secondary parameters                               *
C    9. Amat  -   System state matrix                                *
C                                *
C*****
C#####C

Subroutine SYMBOL
Implicit None

Include 'globals.inc'
Include 'model.inc'

```

```

CC
C-----C
C   Enter as Indicated                               C
C---c-----C

```

```

      NDEqs   = 5   ! Enter # of Diff. Eqs.
      NSParam = 1   ! Enter # of System Parameters.
      NVparam = 2   ! Enter # of Variance Parameters.
      NSecPar = 0   ! Enter # of Secondary Parameters.
      NSecOut = 0   ! Enter # of Secondary Outputs (not used).
      Ieqsol  = 1   ! Model type: 1 - DIFFEQ, 2 - AMAT, 3 - OUTPUT only.
      Descr   = ' DLZ 5CM S1-1 new'

```

```

CC
C-----C
C   Enter Symbol for Each System Parameter (eg. PSym(1)='Kel')   C
C---c-----C

```

```

      PSym(1) = 'Kp'

```

```

CC
C-----C
C   Enter Symbol for Each Variance Parameter {eg: PVsym(1)='Sigma'}   C
C---c-----C

```

```

      PVsym(1)='Intercept'
      PVsym(2)='Sigma'

```

```

CC
C-----C
C   Enter Symbol for Each Secondary Parameter {eg: PSsym(1)='CLt'}   C
C---c-----C

```

```

C-----C
C-----C
C
      Return
      End

C#####C

      Subroutine DIFFEQ(T,X,XP)
      Implicit None

      Include 'globals.inc'
      Include 'model.inc'

      Real*8 T,X(MaxNDE),XP(MaxNDE)
      Real*8 C1,C2,ka,alpha,beta,Cart,Cout1,Cout2,Cout3,Cout4,Cout5
      Real*8 Qliver,Vliver,Kp,Rb,fub,CLint,ER,DN,a,C3,gamma,F,Fi

CC
C-----C
C   Enter Differential Equations Below   {e.g.  XP(1) = -P(1)*X(1) }   C
C---C-----C

      Kp=P(1)
      Qliver=60.82 !mL/min/kg
      Vliver=36.6 !mL/kg
      Rb=0.93
      ER=0.867
      CLint=151.2 ! 5CM SCM

C Fixed parameters:
      C1 = 61990
      C2=1716

```

```

alpha =2.28
beta=0.05659
gamma=0.01052
C3=392.5

```

```

Cart=C1*exp(-alpha*T)+C2*exp(-beta*T)+C3*exp(-gamma*T)  ! blood

```

```

      XP(1)=(Qliver*(Cart-Rb*X(1)/(Kp))
x          -(CLint/5)*Rb*X(1)/(Kp)) / (Vliver/5)

```

```

      XP(2)=(Qliver*(Rb*X(1)/(Kp)-Rb*X(2)/(Kp))
x          -(CLint/5)*Rb*X(2)/(Kp)) / (Vliver/5)

```

```

      XP(3)=(Qliver*(Rb*X(2)/(Kp)-Rb*X(3)/(Kp))
x          -(CLint/5)*Rb*X(3)/(Kp)) / (Vliver/5)

```

```

      XP(4)=(Qliver*(Rb*X(3)/(Kp)-Rb*X(4)/(Kp))
x          -(CLint/5)*Rb*X(4)/(Kp)) / (Vliver/5)

```

```

      XP(5)=(Qliver*(Rb*X(4)/(Kp)-Rb*X(5)/(Kp))
x          -(CLint/5)*Rb*X(5)/(Kp)) / (Vliver/5)

```

```

C-----C
C-----C
C

```

```

      Return
      End

```

```

C#####C

```

```

      Subroutine OUTPUT(Y,T,X)
      Implicit None

```

```

      Include 'globals.inc'

```

```

      Include 'model.inc'

      Real*8 Y(MaxNOE),T,X(MaxNDE)

CC
C-----C
C   Enter Output Equations Below   {e.g.  Y(1) = X(1)/P(2) }   C
C-----C
      Y(1)=X(1)
      Y(2)=X(2)
      Y(3)=X(3)
      Y(4)=X(4)
      Y(5)=X(5)

      Y(6)=(X(1)+X(2)+X(3)+X(4)+X(5))/5

C-----C
C-----C
C
      Return
      End

C#####C

      Subroutine VARMOD(V,T,X,Y)
      Implicit None

      Include 'globals.inc'
      Include 'model.inc'

      Real*8 V(MaxNOE),T,X(MaxNDE),Y(MaxNOE)
      Real*8 Sigma,Intercept

```

```

CC
C-----C
C   Enter Variance Model Equations Below           C
C       {e.g. V(1) = (PV(1) + PV(2)*Y(1))**2 }      C
C-----C-----C
C       Intercept=PV(1)
C       Sigma=PV(2)
C       V(1:6)= (PV(1)+PV(2)*Y(1:6))**2
C-----C-----C
C-----C
C-----C
C
C       Return
C       End

C#####C

C       Subroutine COVMOD(Pmean, ICmean, PC)
C   Defines any covariate model equations (MLEM, ITS)
C       Implicit None

C       Include 'globals.inc'
C       Include 'model.inc'

C       Real*8 PC(MaxNCP)
C       Real*8 Pmean(MaxNSP+MaxNDE), ICmean(MaxNDE)

CC
C-----C
C   Enter # of Covariate Parameters                 C
C-----C-----C

C       NCparam = 0      ! Enter # of Covariate Parameters.

```

```

CC
C-----C
C   Enter Symbol for Covariate Params {eg: PCsym(1)='CLRenal'}      C
C---C-----C

CC
C-----C
C   For the Model Params. that Depend on Covariates Enter the Equation C
C       {e.g. Pmean(1) = PC(1)*R(2) }                                C
C---C-----C

C-----C
C-----C
C
      Return
      End

C#####C

      Subroutine POPINIT(PmeanI,ICmeanI,PcovI,ICcovI, PCI)
C   Initial parameter values for population program parameters (ITS, MLEM)

      Implicit None

      Include 'globals.inc'
      Include 'model.inc'

      Integer I,J
      Real*8 PmeanI(MaxNSP+MaxNDE), ICmeanI(MaxNDE)
      Real*8 PcovI(MaxNSP+MaxNDE,MaxNSP+MaxNDE), ICcovI(MaxNDE,MaxNDE)
      Real*8 PCI(MaxNCP)

```



```

CC
C-----C
C   Enter Initial Values for Population Means           C
C       {   e.g. PmeanI(1) = 10.0       }               C
C-----C-----C

```

```

CC
C-----C
C   Enter Initial Values for Pop. Covariance Matrix (Lower Triang.) C
C       {   e.g. PcovI(2,1) = 0.25       }               C
C-----C-----C

```

```

CC
C-----C
C   Enter Values for Covariate Model Parameters         C
C       {   e.g. PCI(1) = 2.0       }                   C
C-----C-----C

```

```

C-----C
C-----C
C

```

```

    Return
    End

```

```

C#####C

```

```

    Subroutine PRIOR(Pmean,Pcov,ICmean,ICcov)
C   Parameter mean and covariance values for MAP estimation (ID,NPD,STS)
    Implicit None

    Include 'globals.inc'

```

```

      Include 'model.inc'

      Integer I,J
      Real*8 Pmean(MaxNSP+MaxNDE), ICmean(MaxNDE)
      Real*8 Pcov(MaxNSP+MaxNDE,MaxNSP+MaxNDE), ICcov(MaxNDE,MaxNDE)

CC
C-----C
C   Enter Nonzero Elements of Prior Mean Vector      C
C           { e.g. Pmean(1) = 10.0      }           C
C---C-----C

CC
C-----C
C   Enter Nonzero Elements of Covariance Matrix (Lower Triang.)      C
C           { e.g. Pcov(2,1) = 0.25      }           C
C---C-----C

C-----C
C-----C
C

      Return
      End

C#####C

      Subroutine SPARAM(PS,P,IC)
      Implicit None

      Include 'globals.inc'

      Real*8 PS(MaxNSECP), P(MaxNSP+MaxNDE), IC(MaxNDE)
      Real*8 ER,F,Fi,CLinti,CLint

```

```

CC
C-----C
C   Enter Equations Defining Secondary Paramters      C
C           { e.g.  PS(1) = P(1)*P(2)  }              C
C-----C-----C

C-----C
C-----C
C
      Return
      End

C#####C

      Subroutine AMAT(A)
      Implicit None

      Include 'globals.inc'
      Include 'model.inc'

      Integer I,J
      Real*8 A(MaxNDE,MaxNDE)

      DO I=1,Ndeqs
        Do J=1,Ndeqs
          A(I,J)=0.0D0
        End Do
      End Do

CC
C-----C
C   Enter non zero elements of state matrix  {e.g.  A(1,1) = -P(1) }  C
C-----C-----C

```

C-----C  
C-----C  
C

Return  
End

C#####C

**ADAPT code for the zonal SCM (DLZ) (Scenario 1)**

```

*****
C                                ADAPT                                *
C                                Version 5                            *
C*****
C                                *
C                                MODEL                                *
C                                *
C                                *
C    This file contains Fortran subroutines into which the user      *
C    must enter the relevant model equations and constants.          *
C    Consult the User's Guide for details concerning the format for  *
C    entered equations and definition of symbols.                    *
C                                *
C    1. Symbol-   Parameter symbols and model constants              *
C    2. DiffEq-   System differential equations                      *
C    3. Output-   System output equations                            *
C    4. Varmod-   Error variance model equations                    *
C    5. Covmod-   Covariate model equations (ITS,MLEM)              *
C    6. Popinit-  Population parameter initial values (ITS,MLEM)    *
C    7. Prior -   Parameter mean and covariance values (ID,NPD,STS) *
C    8. Sparam-   Secondary parameters                              *
C    9. Amat  -   System state matrix                                *
C                                *
C*****
C#####C

    Subroutine SYMBOL
    Implicit None

    Include 'globals.inc'
    Include 'model.inc'

CC

```

```

C-----C
C   Enter as Indicated                               C
C---C-----C

```

```

NDEqs   = 5    ! Enter # of Diff. Eqs.
NSParam = 1    ! Enter # of System Parameters.
NVparam = 2    ! Enter # of Variance Parameters.
NSecPar = 0    ! Enter # of Secondary Parameters.
NSecOut = 0    ! Enter # of Secondary Outputs (not used).
Ieqsol  = 1    ! Model type: 1 - DIFFEQ, 2 - AMAT, 3 - OUTPUT only.
Descr   = ' DLZ 5CM higher PV '

```

```

CC
C-----C
C   Enter Symbol for Each System Parameter (eg. Psym(1)='Kel')   C
C---C-----C

```

```

      PSym(1) = 'Kp'

```

```

CC
C-----C
C   Enter Symbol for Each Variance Parameter {eg: PVsym(1)='Sigma'}   C
C---C-----C

```

```

      PVsym(1)='Intercept'
      PVsym(2)='Sigma'

```

```

CC
C-----C
C   Enter Symbol for Each Secondary Parameter {eg: PSsym(1)='CLt'}   C
C---C-----C

```

```

C-----C

```

```

C-----C
C
      Return
      End

C#####C

      Subroutine DIFFEQ(T,X,XP)
      Implicit None

      Include 'globals.inc'
      Include 'model.inc'

      Real*8 T,X(MaxNDE),XP(MaxNDE)
      Real*8 C1,C2,ka,alpha,beta,Cart,Cout1,Cout2,Cout3,Cout4,Cout5
      Real*8 Qliver,Vliver,Kp,Rb,fub,CLint,ER,DN,a,C3,gamma,F,Fi
      Real*8 CLint1,CLint2,CLint3,CLint4,CLint5

CC
C-----C
C   Enter Differential Equations Below   {e.g.  XP(1) = -P(1)*X(1) }   C
C---C-----C

      Kp=P(1)
      Qliver=60.82 !mL/min/kg
      Vliver=36.6 !mL/kg
      Rb=0.93
      ER=0.867
      CLint1=4.09
      CLint2=8.454
      CLint3=18.084
      CLint4=41.544
      CLint5=111.467

```

C Fixed parameters:

C1 = 61990  
 C2=1716  
 alpha =2.28  
 beta=0.05659  
 gamma=0.01052  
 C3=392.5

Cart=C1\*exp(-alpha\*T)+C2\*exp(-beta\*T)+C3\*exp(-gamma\*T) ! blood

XP(1)=(Qliver\*(Cart-Rb\*X(1)/(Kp))  
 x - (CLint1)\*Rb\*X(1)/(Kp)) / (Vliver/5)

XP(2)=(Qliver\*(Rb\*X(1)/(Kp)-Rb\*X(2)/(Kp))  
 x - (CLint2)\*Rb\*X(2)/(Kp)) / (Vliver/5)

XP(3)=(Qliver\*(Rb\*X(2)/(Kp)-Rb\*X(3)/(Kp))  
 x - (CLint3)\*Rb\*X(3)/(Kp)) / (Vliver/5)

XP(4)=(Qliver\*(Rb\*X(3)/(Kp)-Rb\*X(4)/(Kp))  
 x - (CLint4)\*Rb\*X(4)/(Kp)) / (Vliver/5)

XP(5)=(Qliver\*(Rb\*X(4)/(Kp)-Rb\*X(5)/(Kp))  
 x - (CLint5)\*Rb\*X(5)/(Kp)) / (Vliver/5)

C-----C  
 C-----C  
 C

Return  
 End

C#####C

Subroutine OUTPUT(Y,T,X)



```
Implicit None
```

```
Include 'globals.inc'
```

```
Include 'model.inc'
```

```
Real*8 Y(MaxNOE),T,X(MaxNDE)
```

```
CC
```

```
C-----C
```

```
C   Enter Output Equations Below   {e.g.  Y(1) = X(1)/P(2) }   C
```

```
C---C-----C
```

```
Y(1)=X(1)
```

```
Y(2)=X(2)
```

```
Y(3)=X(3)
```

```
Y(4)=X(4)
```

```
Y(5)=X(5)
```

```
Y(6)=(X(1)+X(2)+X(3)+X(4)+X(5))/5
```

```
C-----C
```

```
C-----C
```

```
C
```

```
Return
```

```
End
```

```
C#####C
```

```
Subroutine VARMOD(V,T,X,Y)
```

```
Implicit None
```

```
Include 'globals.inc'
```

```

      Include 'model.inc'

      Real*8 V(MaxNOE),T,X(MaxNDE),Y(MaxNOE)
      Real*8 Sigma,Intercept

CC
C-----C
C   Enter Variance Model Equations Below                               C
C       {e.g. V(1) = (PV(1) + PV(2)*Y(1))**2 }                        C
C-----C
C       Intercept=PV(1)
C       Sigma=PV(2)
C       V(1:6)= (PV(1)+PV(2)*Y(1:6))**2

C-----C
C-----C
C
C       Return
C       End

C#####C

      Subroutine COVMOD(Pmean, ICmean, PC)
C   Defines any covariate model equations (MLEM, ITS)
      Implicit None

      Include 'globals.inc'
      Include 'model.inc'

      Real*8 PC(MaxNCP)
      Real*8 Pmean(MaxNSP+MaxNDE), ICmean(MaxNDE)

CC
C-----C

```

```

C      Enter # of Covariate Parameters                                C
C-----C-----C-----C-----C-----C-----C-----C-----C
C
C      NCparam = 0      ! Enter # of Covariate Parameters.
C
CC
C-----C-----C-----C-----C-----C-----C-----C-----C
C      Enter Symbol for Covariate Params {eg: PCsym(1)='CLRenal'}    C
C-----C-----C-----C-----C-----C-----C-----C-----C
C
CC
C-----C-----C-----C-----C-----C-----C-----C-----C
C      For the Model Params. that Depend on Covariates Enter the Equation C
C      {e.g. Pmean(1) = PC(1)*R(2) }                                C
C-----C-----C-----C-----C-----C-----C-----C-----C
C
C-----C-----C-----C-----C-----C-----C-----C-----C
C-----C-----C-----C-----C-----C-----C-----C-----C
C
C      Return
C      End
C#####C
C
C      Subroutine POPINIT(PmeanI,ICmeanI,PcovI,ICcovI, PCI)
C      Initial parameter values for population program parameters (ITS, MLEM)
C
C      Implicit None
C
C      Include 'globals.inc'
C      Include 'model.inc'

```

```

Integer I,J
Real*8 PmeanI (MaxNSP+MaxNDE), ICmeanI (MaxNDE)
Real*8 PcovI (MaxNSP+MaxNDE,MaxNSP+MaxNDE), ICCovI (MaxNDE,MaxNDE)
Real*8 PCI (MaxNCP)

```

```

CC
C-----C
C  Enter Initial Values for Population Means      C
C      { e.g. PmeanI(1) = 10.0      }            C
C----c-----C

```

```

CC
C-----C
C  Enter Initial Values for Pop. Covariance Matrix (Lower Triang.) C
C      { e.g. PcovI(2,1) = 0.25      }            C
C----c-----C

```

```

CC
C-----C
C  Enter Values for Covariate Model Parameters    C
C      { e.g. PCI(1) = 2.0      }                C
C----c-----C

```

```

C-----C
C-----C
C

```

```

Return
End

```

```

C#####C

```

```

      Subroutine PRIOR(Pmean,Pcov,ICmean,ICcov)
C   Parameter mean and covariance values for MAP estimation (ID,NPD,STS)
      Implicit None

      Include 'globals.inc'
      Include 'model.inc'

      Integer I,J
      Real*8 Pmean(MaxNSP+MaxNDE), ICmean(MaxNDE)
      Real*8 Pcov(MaxNSP+MaxNDE,MaxNSP+MaxNDE), ICcov(MaxNDE,MaxNDE)

CC
C-----C
C   Enter Nonzero Elements of Prior Mean Vector      C
C           { e.g. Pmean(1) = 10.0      }           C
C-----C-----C

CC
C-----C
C   Enter Nonzero Elements of Covariance Matrix (Lower Triang.)      C
C           { e.g. Pcov(2,1) = 0.25      }           C
C-----C-----C

C-----C
C-----C
C
      Return
      End

C#####C

      Subroutine SPARAM(PS,P,IC)

```

```
Implicit None
```

```
Include 'globals.inc'
```

```
Real*8 PS(MaxNSECP), P(MaxNSP+MaxNDE), IC(MaxNDE)
```

```
Real*8 ER,F,Fi,CLinti,CLint
```

```
CC
```

```
C-----C
```

```
C   Enter Equations Defining Secondary Paramters      C
```

```
C           { e.g. PS(1) = P(1)*P(2) }                C
```

```
C---C-----C
```

```
C-----C
```

```
C-----C
```

```
C
```

```
Return
```

```
End
```

```
C#####C
```

```
Subroutine AMAT(A)
```

```
Implicit None
```

```
Include 'globals.inc'
```

```
Include 'model.inc'
```

```
Integer I,J
```

```
Real*8 A(MaxNDE,MaxNDE)
```

```
DO I=1,Ndeqs
```

```
  Do J=1,Ndeqs
```

```
    A(I,J)=0.0D0
```

End Do  
End Do

CC  
C-----C  
C Enter non zero elements of state matrix {e.g.  $A(1,1) = -P(1)$  } C  
C---C-----C

C-----C  
C-----C  
C

Return  
End

C#####C

**ADAPT code for the zonal SCM (DLZ) (Scenario 2)**

```

*****
C                                ADAPT                                *
C                                Version 5                            *
C*****
C                                *
C                                MODEL                                *
C                                *
C                                *
C    This file contains Fortran subroutines into which the user      *
C    must enter the relevant model equations and constants.         *
C    Consult the User's Guide for details concerning the format for  *
C    entered equations and definition of symbols.                   *
C                                *
C    1. Symbol-   Parameter symbols and model constants             *
C    2. DiffEq-   System differential equations                     *
C    3. Output-   System output equations                           *
C    4. Varmod-   Error variance model equations                   *
C    5. Covmod-   Covariate model equations (ITS,MLEM)             *
C    6. Popinit-  Population parameter initial values (ITS,MLEM)   *
C    7. Prior -   Parameter mean and covariance values (ID,NPD,STS) *
C    8. Sparam-   Secondary parameters                             *
C    9. Amat  -   System state matrix                               *
C                                *
C*****
C#####C

    Subroutine SYMBOL
    Implicit None

    Include 'globals.inc'
    Include 'model.inc'

CC

```



```

C-----C
C   Enter as Indicated                               C
C---C-----C

```

```

NDEqs   = 5   ! Enter # of Diff. Eqs.
NSParam = 1   ! Enter # of System Parameters.
NVparam = 2   ! Enter # of Variance Parameters.
NSecPar = 0   ! Enter # of Secondary Parameters.
NSecOut = 0   ! Enter # of Secondary Outputs (not used).
Ieqsol  = 1   ! Model type: 1 - DIFFEQ, 2 - AMAT, 3 - OUTPUT only.
Descr   = ' DLZ 5CM higher PP CLint'

```

```

CC
C-----C
C   Enter Symbol for Each System Parameter (eg. Psym(1)='Kel')   C
C---C-----C

```

```

      PSym(1) = 'Kp'

```

```

CC
C-----C
C   Enter Symbol for Each Variance Parameter {eg: PVsym(1)='Sigma'}   C
C---C-----C

```

```

      PVsym(1)='Intercept'
      PVsym(2)='Sigma'

```

```

CC
C-----C
C   Enter Symbol for Each Secondary Parameter {eg: PSsym(1)='CLt'}   C
C---C-----C

```

```

C-----C

```

```

C-----C
C
      Return
      End

C#####C

      Subroutine DIFFEQ(T,X,XP)
      Implicit None

      Include 'globals.inc'
      Include 'model.inc'

      Real*8 T,X(MaxNDE),XP(MaxNDE)
      Real*8 C1,C2,ka,alpha,beta,Cart,Cout1,Cout2,Cout3,Cout4,Cout5
      Real*8 Qliver,Vliver,Kp,Rb,fub,CLint,ER,DN,a,C3,gamma,F,Fi
      Real*8 CLint1,CLint2,CLint3,CLint4,CLint5

CC
C-----C
C   Enter Differential Equations Below   {e.g.  XP(1) = -P(1)*X(1) }   C
C-----C
      Kp=P(1)

      Qliver=60.82 !mL/min/kg
      Vliver=36.6 !mL/kg
      Rb=0.93
      ER=0.867

      CLint1=111.467
      CLint2=41.544
      CLint3=18.084
      CLint4=8.454
      CLint5=4.09

```

C Fixed parameters:

C1 = 61990  
 C2=1716  
 alpha =2.28  
 beta=0.05659  
 gamma=0.01052  
 C3=392.5

Cart=C1\*exp(-alpha\*T)+C2\*exp(-beta\*T)+C3\*exp(-gamma\*T) ! blood

XP(1)=(Qliver\*(Cart-Rb\*X(1)/(Kp))  
 x - (CLint1)\*Rb\*X(1)/(Kp)) / (Vliver/5)

XP(2)=(Qliver\*(Rb\*X(1)/(Kp)-Rb\*X(2)/(Kp))  
 x - (CLint2)\*Rb\*X(2)/(Kp)) / (Vliver/5)

XP(3)=(Qliver\*(Rb\*X(2)/(Kp)-Rb\*X(3)/(Kp))  
 x - (CLint3)\*Rb\*X(3)/(Kp)) / (Vliver/5)

XP(4)=(Qliver\*(Rb\*X(3)/(Kp)-Rb\*X(4)/(Kp))  
 x - (CLint4)\*Rb\*X(4)/(Kp)) / (Vliver/5)

XP(5)=(Qliver\*(Rb\*X(4)/(Kp)-Rb\*X(5)/(Kp))  
 x - (CLint5)\*Rb\*X(5)/(Kp)) / (Vliver/5)

C-----C  
 C-----C  
 C

Return  
 End

C#####C

Subroutine OUTPUT(Y,T,X)

```
Implicit None
```

```
Include 'globals.inc'
```

```
Include 'model.inc'
```

```
Real*8 Y(MaxNOE),T,X(MaxNDE)
```

```
CC
```

```
C-----C
```

```
C   Enter Output Equations Below   {e.g.  Y(1) = X(1)/P(2) }   C
```

```
C---C-----C
```

```
Y(1)=X(1)
```

```
Y(2)=X(2)
```

```
Y(3)=X(3)
```

```
Y(4)=X(4)
```

```
Y(5)=X(5)
```

```
Y(6)=(X(1)+X(2)+X(3)+X(4)+X(5))/5
```

```
C-----C
```

```
C-----C
```

```
C
```

```
Return
```

```
End
```

```
C#####C
```

```
Subroutine VARMOD(V,T,X,Y)
```

```
Implicit None
```

```
Include 'globals.inc'
```

```

      Include 'model.inc'

      Real*8 V(MaxNOE),T,X(MaxNDE),Y(MaxNOE)
      Real*8 Sigma,Intercept

CC
C-----C
C   Enter Variance Model Equations Below                               C
C       {e.g. V(1) = (PV(1) + PV(2)*Y(1))**2 }                        C
C-----C-----C
C       Intercept=PV(1)
C       Sigma=PV(2)
C       V(1:6)= (PV(1)+PV(2)*Y(1:6))**2

C-----C
C-----C
C
C       Return
C       End

C#####C

      Subroutine COVMOD(Pmean, ICmean, PC)
C   Defines any covariate model equations (MLEM, ITS)
      Implicit None

      Include 'globals.inc'
      Include 'model.inc'

      Real*8 PC(MaxNCP)
      Real*8 Pmean(MaxNSP+MaxNDE), ICmean(MaxNDE)

CC
C-----C

```

```

C      Enter # of Covariate Parameters                                C
C-----C-----C-----C-----C-----C-----C-----C-----C
C
C      NCparam = 0      ! Enter # of Covariate Parameters.
C
CC
C-----C-----C-----C-----C-----C-----C-----C-----C
C      Enter Symbol for Covariate Params {eg: PCsym(1)='CLRenal'}    C
C-----C-----C-----C-----C-----C-----C-----C-----C
C
CC
C-----C-----C-----C-----C-----C-----C-----C-----C
C      For the Model Params. that Depend on Covariates Enter the Equation C
C      {e.g. Pmean(1) = PC(1)*R(2) }                                C
C-----C-----C-----C-----C-----C-----C-----C-----C
C
C-----C-----C-----C-----C-----C-----C-----C-----C
C-----C-----C-----C-----C-----C-----C-----C-----C
C
C      Return
C      End
C#####C
C
C      Subroutine POPINIT(PmeanI,ICmeanI,PcovI,ICcovI, PCI)
C      Initial parameter values for population program parameters (ITS, MLEM)
C
C      Implicit None
C
C      Include 'globals.inc'
C      Include 'model.inc'

```

```

Integer I,J
Real*8 PmeanI (MaxNSP+MaxNDE), ICmeanI (MaxNDE)
Real*8 PcovI (MaxNSP+MaxNDE,MaxNSP+MaxNDE), ICcovI (MaxNDE,MaxNDE)
Real*8 PCI (MaxNCP)

```

```

CC
C-----C
C  Enter Initial Values for Population Means      C
C      { e.g. PmeanI(1) = 10.0      }            C
C----c-----C

```

```

CC
C-----C
C  Enter Initial Values for Pop. Covariance Matrix (Lower Triang.) C
C      { e.g. PcovI(2,1) = 0.25      }            C
C----c-----C

```

```

CC
C-----C
C  Enter Values for Covariate Model Parameters    C
C      { e.g. PCI(1) = 2.0      }                C
C----c-----C

```

```

C-----C
C-----C
C

```

```

Return
End

```

```

C#####C

```

```

      Subroutine PRIOR(Pmean,Pcov,ICmean,ICcov)
C   Parameter mean and covariance values for MAP estimation (ID,NPD,STS)
      Implicit None

      Include 'globals.inc'
      Include 'model.inc'

      Integer I,J
      Real*8 Pmean(MaxNSP+MaxNDE), ICmean(MaxNDE)
      Real*8 Pcov(MaxNSP+MaxNDE,MaxNSP+MaxNDE), ICcov(MaxNDE,MaxNDE)

CC
C-----C
C   Enter Nonzero Elements of Prior Mean Vector      C
C           { e.g. Pmean(1) = 10.0           }      C
C-----C-----C

CC
C-----C
C   Enter Nonzero Elements of Covariance Matrix (Lower Triang.)      C
C           { e.g. Pcov(2,1) = 0.25           }      C
C-----C-----C

C-----C
C-----C
C
      Return
      End

C#####C

      Subroutine SPARAM(PS,P,IC)

```



```
Implicit None
```

```
Include 'globals.inc'
```

```
Real*8 PS(MaxNSECP), P(MaxNSP+MaxNDE), IC(MaxNDE)
```

```
Real*8 ER,F,Fi,CLinti,CLint
```

```
CC
```

```
C-----C
```

```
C   Enter Equations Defining Secondary Paramters      C
```

```
C           { e.g.  PS(1) = P(1)*P(2)      }          C
```

```
C---c-----C
```

```
C-----C
```

```
C-----C
```

```
C
```

```
Return
```

```
End
```

```
C#####C
```

```
Subroutine AMAT(A)
```

```
Implicit None
```

```
Include 'globals.inc'
```

```
Include 'model.inc'
```

```
Integer I,J
```

```
Real*8 A(MaxNDE,MaxNDE)
```

```
DO I=1,Ndeqs
```

```
  Do J=1,Ndeqs
```

```
    A(I,J)=0.0D0
```

```
  End Do
```

End Do

CC

C-----C

C Enter non zero elements of state matrix {e.g.  $A(1,1) = -P(1)$  } C

C---c-----C

C-----C

C-----C

C

Return

End

C#####C